MECHANICAL, DIFFUSION AND DEGRADATION BEHAVIOUR OF SAUSAGE FRUIT TREE FIBER (*Kigelia africana*) REINFORCED POLYPROPYLENE COMPOSITES

NZIOKA BEATRICE MUENI (B.Ed. Sc)

I56/CE/28815/2015

A thesis submitted in partial fulfillment of the requirements for the award of degree of Master of Science, in the school of pure and applied sciences of Kenyatta University

APRIL, 2022

DECLARATION

This thesis is my original work and has not been presented for the award of a degree in any other University or any other award.

Signature:…… Date: ……

NZIOKA BEATRICE MUENI

I56/CE/28815/2015

We confirm that the candidate, under our supervision, carried out the work reported in this Thesis.

Signature: …… Date: ……..

DR. ABDALLAH .S. MERENGA

DEPARTMENT OF PHYSICS

KENYATTA UNIVERSITY

Signature: …….. Date: ……..

DR.CHARLES.M. MIGWI

DEPARTMENT OF PHYSICS

KENYATTA UNIVERSITY

DEDICATION

I dedicate this work to my soulmate Edward and my dear son Max Friday.

ACKNOWLEDGMENTS

I thank God for this far he has held my hands in my study. He opened my eyes, empowered my brain and magically influenced everybody around me to give me all the support I needed. I am deeply grateful to everyone who had an input to this thesis. I am grateful to my supervisor, Dr. Merenga Abdallah, for his direction and holdup during my study. His guidance has motivated me to complete this program. I thank Dr. Migwi Charles for his counsel and input was of great worth in my research and thesis write down. I would like to sincerely appreciate my friend and mentor Dr. Zipporah Muthui for her support. My special thanks go to my friends and colleagues: Mrs Mugendi, Yator, Njiru, Nyaga ,Njoroge, Karanja and Kenyatta university lab technicians, for their assistance and support during this program. Finally, I am deeply indebted to my dear husband Edward for his patience, companionship, care, encouragement and deep love throughout. I thank God for my son Max Friday who gave me humble time as I did my work and has been a great inspiration to me. I also deeply appreciate my parents Joseph Nzioka and Justina Mbinya for their encouragement and immense love. Also I thank my siblings for believing in me. Thank you.

TABLE OF CONTENTS

LIST OF TABLES

LIST OF FIGURES

.

ABBREVIATIONS AND ACRONYMS

C_0	Instantaneous creep compliance
C_p	Creep compliance
D	Diffusion coefficient
DMA	Dynamic mechanical analysis
E	Strain
E_a	Activation energy
E_t	Creep modulus at time t
G*	Complex modulus
G’	Storage modulus
G”	Loss modulus
J	Diffusion flux
n	Viscosity
SFTF/PP	Sausage fruit tree fiber-polypropylene
T	absolute temperature
T_g	glass transition temperature
TGA	Thermogravimetric analysis
VFT	Vogel-Fulcher-Tamman
WLF	William-Landel-Ferry
W_{loss}	Weight loss
δ	Phase lag
ε	Creep strain
σ	Stress
τ	Mean relaxation time
τ_0	Pre-exponential factor

ω	Angular frequency

ABSTRACT

Polypropylene is a thermoplastic polymer used in cement mortars, concrete, packaging plastics, and in re-usable containers. It is made from monomer propylene. It is economical and has a good resistance to fatigue in comparison to other polymers. Polypropylene is however non-biodegradable and liable to chain degradation especially in external applications evidenced by cracks and crazing. Previously use of U-V absorbing additives to curb external exposure degradation was increasing on cost and also unfavorable to the environment. The only solution to this is blending polypropylene with natural fiber (cellulose) to modify its structure. PP/Starch blends have poor rigidity, very low thermal stability and high diffusivity. Cellulose is rigid, has high diffusivity and thermal stability hence suitable in reinforcement of polypropylene. Research work is still going on how to improve the mechanical properties and lowering the density of the composites, as well as have biodegradable high performance engineering materials at low cost. This research investigated the mechanical properties, creep, thermal degradation, diffusion and biodegradation measurements of sausage fruit tree fiber reinforced polypropylene composites. Injection molded samples were used, where the fiber was first grinded in to fine powder. Dynamic mechanical analysis was carried out using torsion pendulum at temperature range 30^0 C to 100ºC. Creep measurements were performed at 30, 40, 50 and 60^0C .The time for deformation and recovery of sample was 12 minutes. Diffusion measurements were done at room temperature and mass difference monitored after 7, 30,60, and 90 days. Thermal degradation was done within temperature range 25 to 550^0C at a heating rate 5 ^{o}C/min. Biodegrability was monitored by burying the samples 20 cm under soil. Mass difference monitored after 7, 30,60 ,and 90 days. Cellulose addition in small amounts increased the storage modulus (stiffness) and loss modulus of the polypropylene. Models of analysis for creep data were Burger model and Weibull model. Increase in cellulose loading decreased resistance to creep hence increased deformation. Water intake increased with cellulose loading. Fickian diffusion behavior was noted and diffusion coefficients increased from approximately 1.481×10^{-12} cm^2/s to 1.646×10^{-10} cm^2/s with cellulose loading. Thermal stability of the blends increased with cellulose loading (activation energy increased from approximately 69.22 to approximately 210.01kJ/mol). Biodegradability improved. Lifespan decreased from approximately 199 years for pure polypropylene to approximately 15 years for 20% fiber loading. When polypropylene is reinforced with cellulose the structural rigidity is improved, thermal stability, hydrophilicity and biodegradation increases. Use of SFTF particles in polypropylene matrix should be adopted since these PP blends are promising non-environmental pollutants.

CHAPTER ONE

INTRODUCTION

1.1 Background to the study

Among polymers polypropylene is a commonly used polymer. However, its non-biodegradability, low impact strength and young's modulus properties often limit its applications. Non-biodegradable polymers have attracted much public and industrial research interest because of disposal problems. Besides, solutions of reducing landfills such incineration and recycling, non-biodegradable polymers can be made biodegradable. One way of doing this is to incorporate natural fibers in the polymer to obtain environment friendly composite materials called bio-composites (Alfonso and Roxana, 2003). In the recent past decades, bio composite materials have become popular due to their environmental advantages (Yang *et al*., 2004).

There is increased interest in using natural fibers in polypropylene composites. There exist several historical examples of composites in literature; these include use of bamboo shoots in mud walls, glued woods in walls by Egyptians (1500 BC). Since 1970s, the use of composites had become popular due to development of new fibers such as carbon, boron and aramids and new composite systems with matrices made of metal and ceramics, all synthetic fibers. Artificial fibers are less costly, high tensile strength and excellent insulating properties but non-biodegradable. In the recent past, organic blends have become a strong competitor to inorganic blends due to their low densities, very low cost, non- abrasiveness, recyclability, biodegradability and renewable nature. Studies have shown that stiffness, hardness and biodegradability of

plastics could be improved by incorporation of these organic blends (Hattotuwa *et al*.,2002).

Natural fibers have key advantages over synthetic fibers. The best known renewable resources able to create biopolymer and biodegradable plastics are starch and cellulose (Chandra and Rustgi,1998; Selke, 2000). Environmental advantages such as biodegradability, dynamic properties such as storage modulus, loss modulus and damping behavior and improved thermal stability play a key role in the quality of the final products [Fuad *et al.*, 1994]. In recent past, natural fibers such wood, rice husk, rice straw, wheat, bamboo and banana fibers have been investigated with the aim of reinforcing polypropylene. Natural fiber reinforced polypropylene materials have immense environmental advantages in that they are renewable, less pollutant and reduce green-house emissions, comparatively less costly, available locally, carbon dioxide neutral when burnt and also biodegradable.

Natural fiber reinforced materials are light-weight, tough, low density and good strength. Due to the superiority of natural fiber reinforced polypropylene composites, there is overwhelming demand by consumers and industries for such materials with specific mechanical properties. Rice straw is a natural fiber source for reinforcing polypropylene (Grozdanov, 2006). Rice is a natural fiber of low density 0.480 g/cm^3 (Ismail Ismail et al.,2018)

Addition of rice straw content resulted in increased tensile modulus and the reinforced polypropylene was bio degradable. However, reinforced polymer surface indicated crazing meaning that there was poor fiber matrix adhesion hence rice straw cannot be used as strong reinforcing agent. Also Due to high demand it may not be sufficient to

cater for all natural fiber needs. This has triggered a need for an alternative natural fiber to add to the list of natural fibers that can be used as reinforcement fillers.

This fiber should be cheap, biodegradable, have superior specific mechanical properties like rice straw fiber or even better, have high adhesion with the polymer matrix, and act a strong reinforcing agent. Sausage fruit tree fiber is obtained from sausage tree (*Kigelia africana*), a wild tree that naturally grows in most forests in Kenya. It is a tough tree which is rarely affected by climatic conditions unlike rice. Its fruit is used in brewing traditional beer known as "*Muratina*" in kikuyu and the fiber left thereafter is commonly used as a bathing scourer. Sausage fruit tree fiber also has a low density of 1.316g/cm^3 (Sira and valarmathi et.,2020). The introduction of sausage tree fruit fiber will provide a suitable alternative to rice straw fibers .The purpose of this study was therefore to study the mechanical properties of sausage fruit tree fiber polypropylene composites, thermal properties, decomposition, diffusion and their response on the basis of storage modulus and loss modulus in order to establish whether sausage fruit tree fiber can be used as an alternative source of fiber to reinforce polypropylene materials.

1.2 Statement of the research problem

Most plastics such as polypropylene have many disposal disadvantages ie; non-biodegradable and release toxic fumes on incineration. Use of natural fibers in polypropylene composite has gained popularity in research due to the environmental advantages. There is need for a natural fiber which can be used as a strong reinforcement agent, to simultaneously increase the stiffness and improve the degradability of the composite. Sausage tree fruit fiber is the best candidate in this situation since it is cheap, biodegradable and has a low density of 1.316g/cm^3. This

research has studied on the different proportions in which polypropylene was blended with cellulose fiber to improve its mechanical, diffusion and degradability properties because cellulose is structurally rigid, has low thermal stability, abundant, high diffusivity and has highly polar hydroxyl groups. Upon the exploration, the dynamic mechanical and viscoelastic properties, water infusibility and degradability testing of the polypropylene/cellulose blends were investigated.

1.3 Objectives

1.3.1 General objective

The main objective of this study was to investigate the mechanical, diffusion and degradation properties of sausage tree fruit fiber polypropylene composite.

1.3.2 Specific objectives

(i) Determine the dynamic mechanical properties of PP/STFF composites

(ii) Determine creep (deformation) behavior of PP/STFF composites.

(iii) Determine the thermal degradation in PP/STFF composites

(iv) Determine the diffusion properties in PP/STFF composites

(v) Determine the biodegradability of PP/STFF composites

1.4 Rationale

Polypropylene materials have poor impact toughness and are non- biodegradable while cellulose materials are strong and biodegradable. One way of improving the mechanical, diffusion and degradability properties of polypropylene is by blending with cellulose. This investigation of the mechanical properties of sausage tree fruit fiber reinforced polypropylene confirms whether indeed, sausage fruit tree fiber can be used as a strong and suitable reinforcing agent for polypropylene materials. This

will go a long way in providing an alternative natural fiber for reinforcing polypropylene materials and accelerating its biodegradability, thermal degradability as well as increasing tensile strength.

CHAPTER TWO

LITERATURE REVIEW

Cellulose is among the simplest of the natural polymers that consists of a single repeating unit of D - glucose, linked through carbons 1 and 4 (Reddy and Yang, 2005). Large numbers of graft copolymers of cellulose have been prepared which need modifications of cellulosic fibers for example cellulose acetate grafted with vinyl form a group of biodegradable cellulose (Barbut and Mittal, 1996). The viscoelastic behavior of polypropylene is greatly affected by the presence of cellulose fibers. An increase in the storage (E') modulus and reduced damping values can be observed with increasing fiber content due to reinforcing effect and interfacial adhesion between fibers and matrix (Amash and Zugenmaier, 1999).

The linear mechanical properties above the glass- rubber transition of Nano composite film of isotactic polypropylene reinforced with cellulose whiskers are drastically enhanced as compared to the neat polypropylene matrix (Ljunberg et al.,2006). Rice straw is a good natural fiber source for reinforcing polypropylene (Grozdanov,2006). Investigation of mechanical properties of the PP/rice straw composites show that rice straw can be used as reinforcement for polypropylene. The addition of rice straw content resulted in increased tensile modulus though there is weak adhesion between rice straw filler and polymer matrix. Guo and coworkers investigated the effects of compatibilizer including maleic anhydride grafted polypropylene (MA-PP) and maleic anhydride grafted ethylene-propylene-dine copolymer (MAEPDM) on wood-floor/polypropylene (WF/PP) composites. Dynamic mechanical analysis showed that the loss factor of composites decreased and the storage modulus improved in the

presence of MA-PP (Guo *et al.,* 2006). The use of polypropylene in-reactor alloys has led to increased interests of scientific and industrial research due to the superior mechanical properties and favorable cost (Rongbo *et al.,* 2009).

Blending PP with cellulose from acacia lowers the storage modulus and improves diffusion properties. Higher content of cellulose in PP matrix showed more biodegradation in the PP blends than pure PP promising non-environmental pollutants (Kiprono *et al.,*2013). The act of heat or raised temperature on a material to cause a harm of physical, mechanical or electrical properties or all is referred to as thermal degradation. Through the use of thermogravimetric analyzer (TGA) in kinetic studies, the evaporation rate of product is determined and not the internal chemical reaction rate, since not every broken-bond in the polymer chain leads to the evaporation of the products. Only product fragments which are small enough to evaporate will actually evaporate at a given reaction temperature and thus leads to a decrease of the polymer mass [Weterhout *et al*., 1997].

Introduction of natural fibers to polymer reduce drastically the amount of combustible gases and favor the formation of carbonaceous char and water. Unrestrained burning of polypropylene causes air pollution and environmental problems due production of toxic gases [Dimitrova *et al*., 2008]. Use of polypropylene bio composites made using natural fiber has been increasing in recent past in electrical and automotive engineering owing to their admirable storage modulus (stiffness). This renders conventional materials like glass fibers conquered.

The main benefit of bio-composites above glass fiber composites is upon incineration there is less amount of toxic residue. The use of bio-composites has unending environmental advantages [Broge, 2000]. Properties of natural fiber composite systems such as dynamic properties like damping behavior and thermal properties have an effect in the quality of the ultimate products. For instance, high temperatures during a hot shower increases the polymer chain mobility of the bathroom interiors leading to deformation, while during summertime temperature inside the vehicle affect the dashboards leading to thermal deformation. It is crucial to note that the strength of these systems is helpful in case of fire outbreak. This is due to the fact that these materials must stand the heat [Khalid *et al.,* 2009].

Optimization of application of PP leads to many of its commercial grades containing fillers or fibers to improve rigidity. Regrettably shots to use wood in such materials ended up unproductive, although the rigidity of the material got to preferred levels, its impact resistance stayed consistently minor and the adhesion in the matrix was poor. The deformability of bio-composites is very essential for real life applications. Reinforcing fibers raise the rigidity of the composites, often resulting in very stiff materials with poorer impact properties. (R. Vardai, et al.,2019).

Despite the research that has been done on polypropylene and cellulose, investigations on the mechanical, biodegradability, thermal degradation and diffusion analysis of sausage fruit tree fiber reinforced polypropylene have not been done yet. This research is intended to give an insight into the mechanical, biodegradability, thermal degradation and sorption properties of PP/SFTF composites

CHAPTER THREE

THEORETICAL BACKGROUND

3.1 Introduction

This chapter gives the related theory applied in this thesis giving an insight on dynamic mechanical properties, linear viscoelasticity, creep behavior, thermogravimetric properties, diffusion and biodegradability of polypropylene. The first polypropylene resin was produced by Guilin Natta in Spain, although commercial production began in 1957. It is manufactured from propylene gas in the presence of a catalyst such as titanium chloride. PP is a by-product of oil refining processes (Lenntech, 1998). Most polymers are very durable, however, can be made to degrade photo-chemically by incorporation of carboxyl groups that absorb ultra-violet radiation to form excited states that are energetic enough to undergo bond cleavage (Gindl. 2006).

3.2 Creep models

NFPCs have high creep resistance under constant stress which is a desirable quality in construction materials. The bending of a sample exposed to unchanging load, which depends on period, temperature and properties of the sample, is known as creep. Creep deformation can go beyond the usual creep and cause permanent deformation of product if the material is subjected to long term load. For application purposes, perception, examination and prognosis of creep behaviors of NFPCs is of great significance [Park and Balatinez, 1997]. In polymeric materials, creep process is divided into four stages: instantaneous deformation, primary creep, secondary creep and tertiary creep. When stress is applied, the instantaneous deformation is caused by

the elastic deformation of the sample. This is trailed by creep rate that begins at a great value and drops steadily to a comparatively smaller value, the primary creep stage. In the secondary creep stage, the creep rate remains constant because of viscous flow.

Creep finally gets to the tertiary stage with swelling creep until creep break out happens [Yang *et al.,* 2004].Viscoelastic characteristics of polymers can be well understood by studying the stress response of mechanical models using an ideal spring as the element that obeys hookes' law and a dashpot as the viscid element. These models consist of a series of a spring and dashpot, the Maxwell element and a parallel combination of a spring and a dashpot, the Voigt element (David Roylance. 2001), as in Figure. 3.1

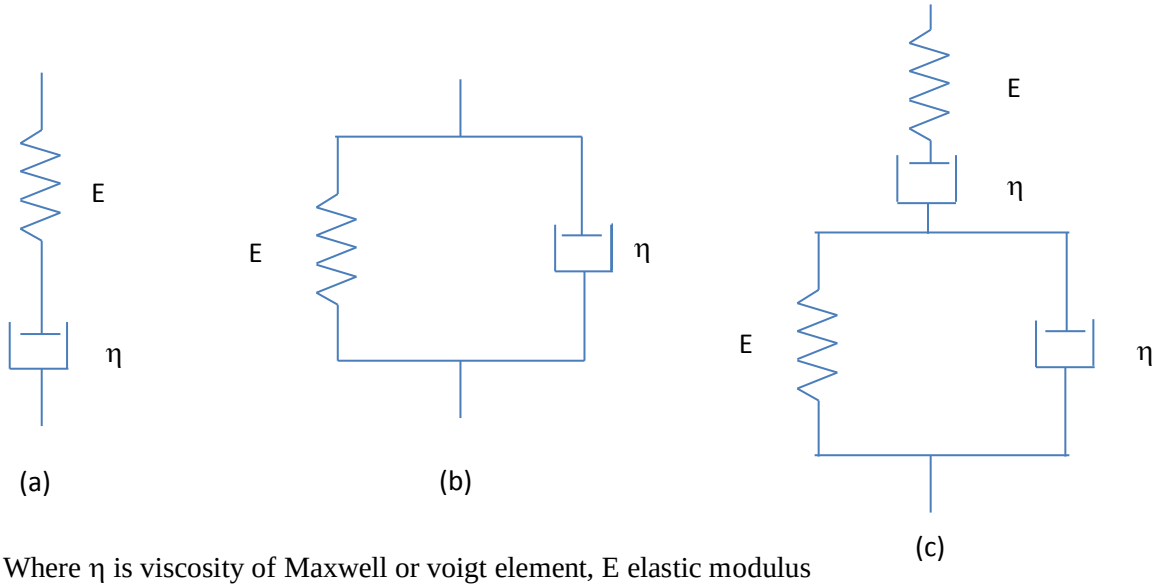

Where η is viscosity of Maxwell or voigt element, E elastic modulus

Figure3.1 (a) Maxwell, (b) Voigt and (c) Burger elements

3.2.1 Maxwell Model

In the case of Figure 3.1 (a) the total strain (or strain rate) is the sum of the discrete strains of the spring and dashpot. From Hooke's law ($\sigma = E\varepsilon$), the strain rate for the spring is

$$\frac{d\varepsilon}{dt} = \frac{1}{E}\frac{d\sigma}{dt} \tag{3.1}$$

From Newton's law of viscosity ($\eta = \sigma / (d\varepsilon/dt)$), the strain rate for the dashpot is

$$\frac{d\varepsilon}{dt} = \frac{\sigma}{\eta} \tag{3.2}$$

Summing the two strain rates give

$$\frac{d\varepsilon}{dt} = \frac{1}{E}\frac{d\sigma}{dt} + \frac{\sigma}{\eta} \tag{3.3}$$

In creep deformation, a constant stress σ_o is applied instantaneously reducing equation 3.3 to

$$\frac{d\varepsilon}{dt} = \frac{\sigma_o}{\eta} \tag{3.4}$$

Rearranging and integrating equation 3.4 gives

$$\int_{\varepsilon_o}^{\varepsilon} d\varepsilon = \frac{\sigma_o}{\eta}\int_o^t dt \qquad \varepsilon(t) = \frac{\sigma_o t}{\eta} + \varepsilon_o = \frac{\sigma_o}{E} + \frac{\sigma_o t}{\eta} = \sigma_o\left(\frac{1}{E} + \frac{t}{\eta}\right) \tag{3.5}$$

where ε_o is the instantaneous strain response of the spring element. The creep compliance is given by

$$C(t) = \frac{\varepsilon(t)}{\sigma_o} = \frac{t}{\eta} + \frac{\varepsilon_o}{\sigma_o} = \frac{t}{\eta} + C_o = C_o\left(\frac{t}{\eta C_o} + 1\right) = C_o\left(\frac{t}{\tau} + 1\right) \tag{3.6}$$

where τ is the relaxation time which is the measure of how quickly a material recovers. The time taken for the stress to fall to a value 1/2.7 of the original stress.

In an experiment stress withdrawal (creep recovery), εo is constant and $d\varepsilon/dt = 0$, and equation 3.3 becomes

$$\frac{1}{\mathrm{E}}\frac{\mathrm{d}\sigma}{\mathrm{dt}} + \frac{\sigma}{\eta} = 0 \tag{3.7}$$

Rearranging and introducing τ gives

$$\int_{\sigma_o}^{\sigma} \frac{\mathrm{d}\sigma}{\sigma} = -\frac{1}{\tau}\int_0^t dt \tag{3.8}$$

Integration yields the stress response

$$\sigma = \sigma_o exp\left(-\frac{t}{\tau}\right) \tag{3.9}$$

The stress relaxation modulus is

$$E_r = \frac{\sigma}{\varepsilon_o} = \frac{\sigma_o}{\varepsilon_o} exp\left(-\frac{t}{\tau}\right) = Eexp\left(-\frac{t}{\tau}\right) \quad (3.10)$$

3.2.2 Voigt Model

The strain in each element Figure 3.1(b) must be identical while the stress is cumulative. Thus

$$\sigma = E\varepsilon + \eta\frac{d\varepsilon}{dt} \quad (3.11)$$

Using τ in creep deformation

$$\frac{\sigma_o}{\eta} = \frac{\varepsilon(t)}{\tau} + \frac{d\varepsilon(t)}{dt} \quad (3.12)$$

Integrating gives

$$\frac{E}{\eta}\int_0^t dt = \int \frac{d\varepsilon}{\frac{\sigma}{E}-\varepsilon}$$

$$\frac{t}{\tau} = ln\left(\frac{\sigma/E}{\frac{\sigma}{E}-\varepsilon}\right)$$

$$\varepsilon e^{t/\tau} = \frac{\sigma}{E}\left(e^{t/\tau} - 1\right)$$

$$\varepsilon(t) = \frac{\sigma}{E}\left(1 - e^{t/\tau}\right) \quad (3.13)$$

3.2.3 Burgers model

This is the sum of Maxwell and Voigt elements in series. Adding equations 3.5 and 3.13 the rate of creep strain is

$$\varepsilon(t) = \sigma_o\left(\frac{1}{E} + \frac{t}{\eta}\right) + \frac{\sigma_o}{E}\left(1 - e^{t/\tau}\right) = \frac{\sigma_o}{E_M} + \frac{\sigma_o}{E_k}\left(1 - e^{t/\tau}\right) + \frac{\sigma_o t}{\eta_M} \quad (3.14)$$

Where E_M is the instantaneous elastic modulus, E_K is the delayed elastic modulus ,σ_0 is the constant applied stress, η_M is viscosity of the Maxwell element and η_K is viscosity of the kelvin dashpots. These are the parameters necessary for describing generalized burgers model.

3.2.4 Weibull distribution model

Weibull proposed a statistical distribution function demonstrating its wide applicability by testing the function with data from broad field of subject areas (Kevin s. Fancey. 2001). The cumulative distribution in terms of time t, F(t):

$$F(t) = 1 - exp\left[-\left(\frac{t-\gamma}{\eta}\right)^{\beta}\right] \quad (3.15)$$

The parameter γ represents the time at which F(t)=0, η is the characteristic life and β the shape parameter. F(t) represents the proportion of elements within a population that have failed by time t. Therefore, the proportion of elements surviving to time t will be 1-F(t), which is defined as R(t). thus:

$$R(t) = exp\left[-\left(\frac{t-\gamma}{\eta}\right)^{\beta}\right] \quad (3.16)$$

Figure 3.2 below show a simple mechanical representation of a spring- dashpot latch model. The latches are fully extended in figure 3.2 (a) and, during recovery fig 3.2(b), a latch is considered to have failed once it has been triggered(Kevin s. Fancey. 2001).

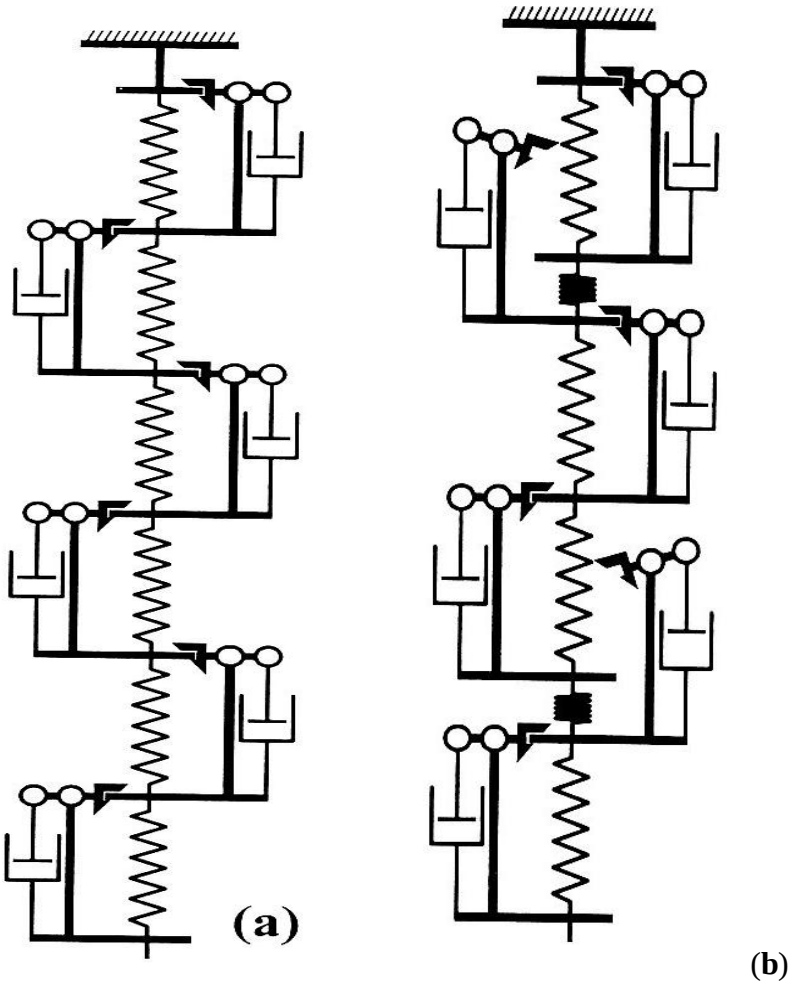

Figure 3.2: A spring- dashpot latch model to represent viscoelastic recovery. All the latch elements are fully extended in (a) and partial recovery of the strain is shown in (b).

Viscoelastic recovery in a real polymeric material would be represented by many latch elements giving a distribution of trigger times. The latch model characteristics maybe represented by equations 3.15 and 3.16 in the same way reliability engineering considers the failure of elements within a system. A similar argument can be proposed for polymeric creep. Here the applied load will cause the progressive activation of latch elements. The activation process could be represented by spring-dashpot controlled triggering, comparable to that depicted in figure 3.2(Kevin s. Fancey. 2001). The action of triggering a latch under these conditions can be though to represent a failure or perhaps more logically, a “birth”. Clearly, it can be argued that

some latches activated under creep conditions may, during recovery, have trigger times that approach infinity. These elements would represent viscous flow in the polymer.

Figure 3.3 shows the components assumed to represent strain in polymeric creep-recovery cycle.

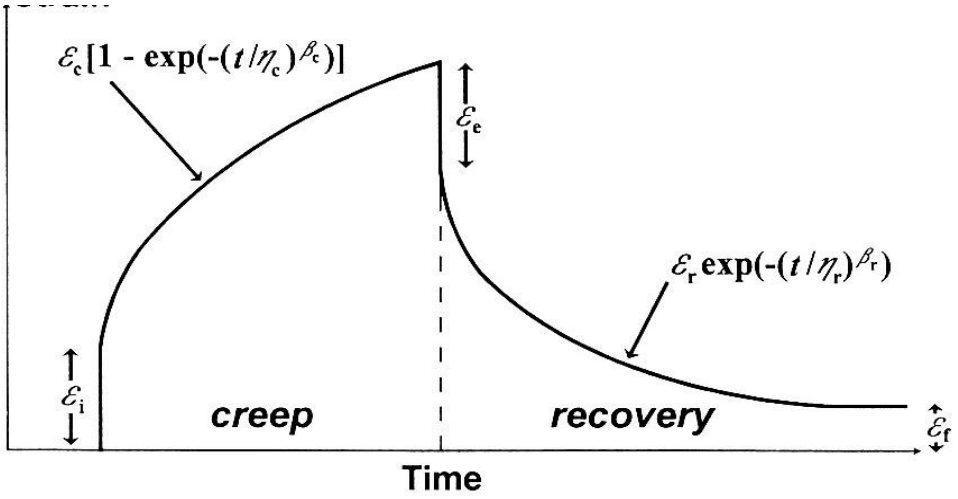

Figure 3.3: The polymeric creep- recovery cycle (schematic) with proposed strain components.

The creep strain ε_c is associated with equation 3.15 to represent the cumulative number of activations with time, whereas the viscoelastic recovery strain εr is associated with equation 3.16 to represent survival: This maintains convection by ensuring that shape parameter will be positive in both cases. For simplicity, γ from equation 3.15 and 3.16 is set to zero where η represents the time when R(t) reaches e^{-1} (i.e. 36.8%)or when 63.2% of the elements have failed. This is independent of β. Any instantaneous strain from initial application of the load for causing creep is represented by ε_i thus the total strain under applied load is:

$$\varepsilon_e tot(t) = \quad \varepsilon_i + \varepsilon_e \left[1 - exp\left(-\frac{t}{\eta_e}\right)^{\beta_e}\right] \qquad (3.17)$$

When the load is removed, there may be some instantaneous (elastic) recovery, ε_e before the onset of viscoelastic processes. The remaining contribution from viscoelasticity (Recovery strain) ε_r and viscous flow, ε_f is:

$$\varepsilon_r(t) = \varepsilon_r\left[exp\left(-\frac{t}{\eta_r}\right)^{\beta_r}\right] + \varepsilon_f \qquad (3.18)$$

Where β_r is shape parameter or Weibull slope, ε_r is strain after short time, ε_f is strain after long time ,η_r is characteristic life parameter.

3.3 Dynamic mechanical analysis

3.3.1 Dynamic mechanical model

To attain the equation for the dynamic mechanical response i.e complex modulus, the equation of complex stress $\sigma = \sigma_o \exp(i\omega t)$, is substituted into equation 3.3 to give

$$\frac{d\varepsilon(t)}{dt} = \frac{1}{E}\frac{d}{dt}\left(\sigma_o e^{i\omega t}\right) + \frac{1}{\eta}\left(\sigma_o e^{i\omega t}\right) = \frac{\sigma_o}{E} i\omega e^{i\omega t} + \frac{\sigma_o}{\eta} e^{i\omega t} \qquad (3.19)$$

Integrating from time t_1 to t_2 gives

$$\int_{t_1}^{t_2} d\varepsilon = \frac{\sigma_o}{E} i\omega \int_{t_1}^{t_2} e^{i\omega t} dt + \frac{\sigma_o}{\eta}\int_{t_1}^{t_2} e^{i\omega t} dt \qquad (3.20)$$

Hence,

$$\varepsilon(t_2) - \varepsilon(t_1) = \frac{\sigma_o}{E}\left(e^{i\omega t_2} - e^{i\omega t_1}\right) + \frac{\sigma_o}{\eta i\omega}\left(e^{i\omega t_2} - e^{i\omega t_1}\right) \qquad (3.21)$$

And the corresponding stress increment is

$$\sigma(t_2) - \sigma(t_1) = \sigma_o\left(e^{i\omega t_2} - e^{i\omega t_1}\right) \qquad (3.22)$$

Dividing equation 3.21 by 3.22 and using τ, gives the complex creep compliance as

$$C^*(\omega) = C(t_2) - C(t_1) = \frac{1}{E} + \frac{1}{\eta i\omega} = \frac{1}{E} + \frac{i}{\eta\omega} = C - \frac{iC}{\omega\tau} = C'(\omega) + iC"(\omega) \qquad (3.23)$$

The equivalent expression for complex modulus E^*, is given by

$$E^*(\omega) = \frac{1}{C^*(\omega)} = \frac{1}{C - \frac{iC}{\omega\tau}} = \frac{\left(C + \frac{iC}{\omega\tau}\right)}{\left(C - \frac{iC}{\omega\tau}\right)\left(C + \frac{iC}{\omega\tau}\right)} \qquad (3.24)$$

Using E=1/C, gives

$$E^*(\omega) = E' + iE'' = \frac{E(\omega\tau)^2}{1+(\omega\tau)^2} + i\left[\frac{E\omega\tau}{1+(\omega\tau)^2}\right] \quad (3.\ 25)$$

Where the real and imaginary parts are the storage and loss moduli, Figure. 3.4 illustrates the two.

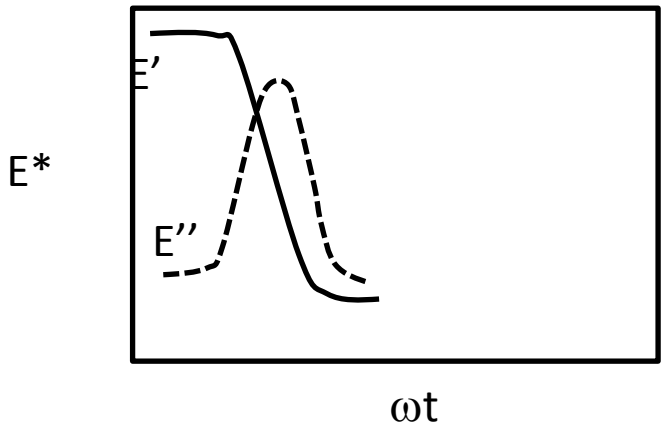

Figure 3.4: Complex modulus and its components

3.3.2 Temperature dependence of relation models

For local chain motion free volume is unnecessary and temperature dependence of relaxation is given by Arrhenius law

$$\tau = \tau_o exp\left[\frac{E_a}{kT}\right] \quad (3.\ 26)$$

Where τ_o and E_a are pre-exponential factor and activation energy respectively.

For main chain motion free volume is necessary and relaxation time is given by Doolittle equation

$$\tau = \tau_o exp\left[B\left(\frac{1}{\phi} - 1\right)\right] \quad (3.\ 27)$$

Where $\phi = (v\text{-}v_o)/v_o$, v_o being the occupied volume, B is a constant and v is free volume which is a function of temperature or

$$v = v_o + \alpha(T - T_o) \quad (3.\ 28)$$

Where α is the expansion coefficient. Substituting for ϕ and $v\text{-}v_o$ into equation 3.27 gives the Vogel-Fulcher-Tamman law (Vogel, 1921)

$$\tau = \tau_o exp\left[\left(\frac{B[v_o - \alpha(T-T_o)]/\alpha}{T-T_o}\right)\right] = \tau_o exp\left[\frac{m}{T-T_o}\right] \quad (3.29)$$

Where T_o is Vogel temperature which is 50^oC below T_g and $m = Bv_o/\alpha$.

Taking natural logarithm of eq. 3.27 gives

$$ln(\tau) = ln(\tau_o) + B\left(\frac{1}{\phi} - 1\right) \quad (3.30)$$

The corresponding equation for T_g is then

$$ln(T_g) = ln(\tau_o) + B\left(\frac{1}{\phi_g} - 1\right) \quad (3.31)$$

The temperature dependence of fractional free volume ϕ is given by

$$\phi = \phi_o + \alpha(T - T_g) \quad (3.32)$$

The shift factor can be defined as

$$a_T = \frac{\tau}{\tau_{T_g}} \quad (3.33)$$

Taking natural logarithm gives

$$ln(a_T) = ln(\tau) - ln\left(\tau_{T_g}\right) \quad (3.34)$$

Substitution of eq. 3.30 and 3.31 into eq. 3.34 gives

$$ln(a_T) = ln(\tau_o) + B\left(\frac{1}{\phi} - 1\right) - \left[ln(\tau_o) + B\left(\frac{1}{\phi_g} - 1\right)\right] = B\left(\frac{1}{\phi} - \frac{1}{\phi_g}\right) \quad (3.35)$$

Since $ln(a_T) = 2.303log(a_T)$ eq. 3.35 gives

$$log(a_T) = \frac{B}{2.303}\left(\frac{1}{\phi_o + \alpha(T - T_g)} - \frac{1}{\phi_g}\right) = \frac{B}{2.303}\left(\frac{-\alpha(T - T_g)}{\phi_o + \alpha(T - T_g)}\right) = \frac{-B}{2.303}\left(\frac{(T - T_g)}{\phi_o/\alpha + (T - T_g)}\right) \quad (3.36)$$

If we let C_1 = -B/2.303 and $C_2 = \phi_o/\alpha$ the William-Lendl-Ferry equation is obtained

$$log(a_T) = \frac{C_1(T - T_g)}{C_2 + T - T_g} \quad (3.37)$$

The temperature dependence of relaxation processes can be illustrated in an activation plot shown in Figure. 3.5

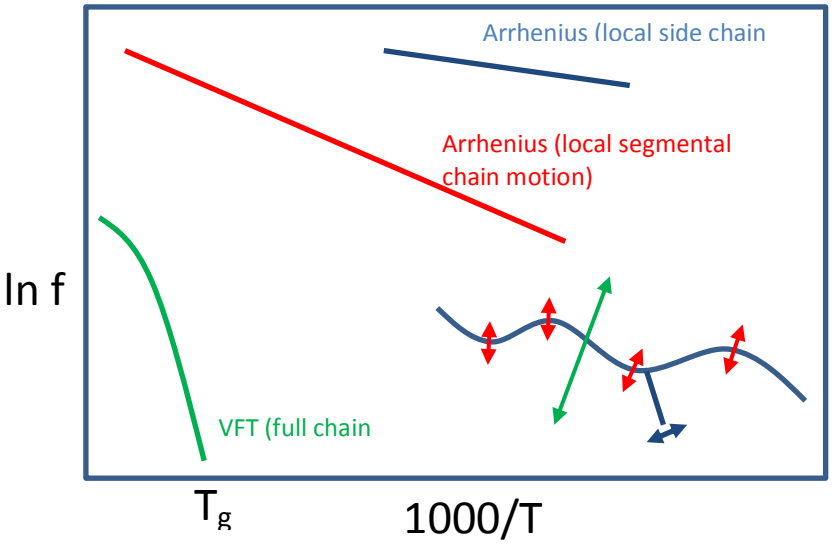

Figure 3.5: A plot of logarithm of frequency against reciprocal temperature

3. 3.3 Loss modulus model

The loss modulus measured in DMA experiment can be expressed as 3.38

$$E''(T) = A\,exp\left\{-\frac{E_a}{kT} - \frac{B}{b}\int_{T_0}^{T} exp\left[-\frac{E_a}{kT}\right]dT\right\} \qquad (3.\ 38)$$

Where T_0 , b , A, B and E_0 are the initial temperature, heating rate, constants and activation energy, respectively. Below T_g relaxation time is governed by Arrhenius law (3.39)

$$\tau(T) = \tau_0 exp\left[-\frac{E_a}{kT}\right] \qquad (3.\ 39)$$

Above T_g , relaxation time is governed by vogel-Fulcher- Tamman law 3.29 or

$$\tau(T) = \tau_0 \tau exp\left[-\frac{E_a}{k(T-T_i)}\right] \qquad (3.\ 40)$$

Where T_i is the vogel temperature which is 50^0C below T_g . Generally, the integral is approximated as equation 3.41

$$ln[E''(T)] = \ln A - f - \frac{BT}{bf}\left(1 - \frac{2!}{f} + \frac{3!}{f} + \frac{4!}{f} + \cdots\right)\exp(-f) \qquad (3.\ 41)$$

Where $f = (\frac{E_a}{kT})$ a better approximation for eqn 3.38 is

$$ln[E''(T)] = \ln A - f - \{\frac{BT}{bf}\left(1 - \frac{2!}{f} + \frac{3!}{f} + \frac{4!}{f} + \cdots\right)\exp(-f)\} \quad (3.42)$$

Where $f = (\frac{E_a}{kT})$ for peaks below T_g above which $f = (\frac{E_a}{k(T-T_i)})$ and B is given by

$$B = \frac{bE_a}{kT_m^2}\ exp\left[-\frac{E_a}{kT_m}\right] \quad (3.43)$$

Where T_m corresponds to temperature corresponding to maximum loss modulus. Considering only the first term in the expression of the integral in equation 3.38, along with equation 3.43, the loss modulus is given by

$$E''(T) = A\ exp\left\{-\frac{E_a}{kT} - \frac{T^2}{T_m^2} exp\left[\frac{E_a}{k}\left(\frac{1}{T_m} - \frac{1}{T}\right)\right]\right\} \quad (3.44)$$

Using equation 3.44, the loss modulus corresponding to the peak maximum is approximately

$$E''(T) = Aexp\left(-\frac{E_a}{kT_m} - \frac{1}{T}\right) \quad (3.45)$$

3.4 Diffusion models

The quantity of an element transported within another is a function of time. Considering a sample of capacity in the form of a four-sided solid whose sides are parallel to the axes of coordinates and are of lengths 2dx,2dy, 2dz. Let the middle of the sample be at M(x,y,z), and the concentration of difusant be C. let PQRS and P'Q'R'S' be the faces at right angles to the axis of x as in figure 3.6.Then the speed at which difusant go into the element via the face PQRS in the plane x-dx is given by

$$4dydz\left(F_x - \frac{\partial F_x}{\partial x}\ dx\right) \quad (3.46)$$

Where F_x is the rate of transfer through the unit area of the corresponding plane through Similarly the rate of loss of diffusing substance through the face P'Q'R'S' is given by $4dydz\left(F_x + \frac{\partial F_x}{\partial x}\, dx\right)$

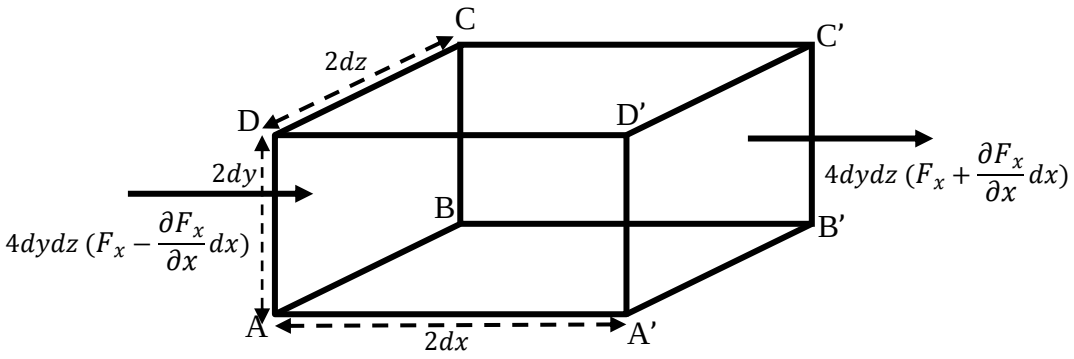

Figure 3.6: Diffusion through free volume.

The involvement of the amount of diffusing matter per unit time in to the sample from the two faces is equivalent to

$$-8dxdydz\left(\frac{\partial F_x}{\partial x}\right) \qquad (3.\ 47)$$

Similarly, from the other faces we obtain

$$-8dxdydz\left(\frac{\partial F_y}{\partial y}\right) \qquad and \qquad -8dxdydz\left(\frac{\partial F_z}{\partial z}\right) \qquad (3.48)$$

But the rate at which the amount of diffusing substance in the sample increases is also given by

$$8dxdydz\left(\frac{\partial C}{\partial t}\right) \qquad (3.49)$$

And hence we have immediately

$$\frac{\partial C}{\partial t} + \frac{\partial F_x}{\partial x} + \frac{\partial F_y}{\partial y} + \frac{\partial F_z}{\partial z} = 0 \qquad (3.50)$$

If the diffusion coefficient is constant, F_x, F_y, F_z are given by 3.51 and 3.52 becomes

$$\frac{\partial C}{\partial t} = D\left(\frac{\partial^2 C}{\partial x^2} + \frac{\partial^2 C}{\partial y^2} + \frac{\partial^2 C}{\partial z^2}\right) \quad (3.51)$$

Reducing simply

$$\frac{\partial C}{\partial t} = -D\left(\frac{\partial^2 C}{\partial x^2}\right) \quad (3.52)$$

If diffusion takes place in one –dimension i.e. if by the x-axis there is a concentration gradient. Equation 3.50 is known as Fick's first law of diffusion while 3.52 is known as Fick's second law of diffusion (Fick 1885).

3.4.1 Concentration-depended diffusion coefficient

Provided that diffusion coefficient (D) changes with concentration(C), then the value of diffusion coefficient obtained from a measurement where the conditions at all points in the element remain constant as time changes is an average value of the concentration. Hence, if D is a function of C then

$$\frac{\partial}{\partial x}\left(D\frac{dC}{dx}\right) = 0$$

And hence the relationship

$$F = -D\,{}^{dC}/_{dx} = constant \quad (3.53)$$

is still valid, since it is requisite to be in the steady state. Integrating between the two surface concentrations C_1 and C_2, we have

$$F = -\frac{1}{l}\int_{c_1}^{c_2} D\,dC = D_1(C_1 - C_2)/l \quad (3.54)$$

where

$$D_1 = \frac{1}{C_1 - C_2} \int_{C_2}^{C_1} D dC \qquad (3.55)$$

this is the average value obtained from a measurement of F. Then, if D depends on C, the concentration nonlinearly depends on the diffusion distance across the membrane.

3.4.2 Non- steady state

Equations here can be attained by both the Laplace transform method and method of separation of variables. Most outcomes are cited by Barrer(1951), Jacobs (1967), and others. Most weight here is on numerical valuation.

Constants of surface concentrations. Preliminary distribution f(x) if

$C=C_1$, x=0, t≥0, (3.56)

$C=C_2$, x=l , t≥0 (3.57)

C=f(x), 0< x >l, t=0, (3.58)

The solution in the form of triangular series is

$$C = C_1 + (C_2 - C_1)\frac{x}{l} + \frac{2}{\pi}\sum_1^\infty \frac{C_2 \cos n\pi - C_1}{n} \sin\frac{n\pi x}{l} exp(-Dn^2\pi^2/l^2) + \frac{2}{l}\sum_1^\infty \sin\frac{n\pi x}{l} exp(-Dn^2\pi^2/l^2) \int_0^1 f(x')\sin\frac{n\pi x'}{l} dx \qquad (3.59)$$

In most cases of incidence f(x) is null or continual in that the integral in equation 3.59 can easily be solved. Frequently, the problem is uniform around the middle plane of the sample. The equations then most reliable if the surfaces are taken as x=±1and the middle plane is taken as x=0.

3.4.3 Uniform initial distribution. Equal Surface concentrations

This is the adsorption and desorption by film. If the region -1< x >l is at uniform initial concentration C_0, and the sides are maintained at uniform concentration c_1, the solution of equation 3.59 turns out to be

$$\frac{C-C_0}{C_1-C_0} = 1 - \frac{4}{\pi}\sum_{n=0}^{\infty}\frac{(-1)^n}{2n+1} exp\{-D(2n+1)^2\pi^2 t/4l^2\} Cos\frac{(2n+1)\pi x}{2l} \qquad (3.\ 60)$$

If m_t denotes the amount of diffusing substance which has entered the sheet at time t, and m_{max} the corresponding quantity after infinite time, then

$$\frac{M_t}{M_{max}} = 1 - \sum_{n=0}^{\infty}\frac{8}{(2n+1)^2\pi^2} exp\left[\frac{-D(2n+1)^2\pi^2 t}{4l^2}\right] \qquad (3.61)$$

The value of diffusion coefficient can be evaluated from the initial stages of the slope of the graph of M_t/M_{max} against $t^{½}$

For the process that takes place at short time (For values of M_t/M_{max} lower than 0.5), equation 3.61 can be written, for thickness of L=2l as;

$$\frac{M_t}{M_{max}} = \frac{2}{l}\left(\frac{D}{\pi}\right)^{1/2} t^{1/2} \qquad (3.62)$$

where M_t is the relative mass uptake at a time, t, M_{max} is the mass uptake at equilibrium, *l* is the film thickness and D is diffusion coefficient.

3.5 Thermal degradation model

Thermal degradation of polymers is the breakdown of the molecular structure as a result of 'overheating'. At high temperatures the components of the long chain backbone of the polymer can begin to separate (molecular scission) and react with one another to change the properties of the polymer. When a polymer material degrades, its mass decreases. This kind of general reaction is expressed in equation 3.63 below

$$S(s) = P_1\ (s) + P_2\ (s) \quad (3.63)$$

The disappearance rate of the species (S) can be calculated as follows:

$$\frac{dx}{dt} = -kx^n \quad (3.64)$$

with S(s) the reactant, P1(s) and P2(s) the remainder and gaseous product, k – the rate constant

$$k = Ze^{-E_a/RT} \quad (3.65)$$

Which obeys the Arrhenius equation for the early stage of the reaction, Z is the frequency factor, considering that temperature increases linearly with time in this experiment,

$$T = T_0 + \beta t \quad (3.66)$$

Where β is the rate of heating, and T_0 is the beginning temperature. Combining equations 3.64, 3.65 and 3.66 gives

$$\frac{dx}{x^n} = -\left(Z/\beta\right) e^{-E_a/RT}\, dt \quad (3.67)$$

The thermogravimetric analysis curve for such a reaction depicts equation 3.67 integrated from a temperature T_0 at which *y=1*. Thus,

$$\int_y^1 dx/x^n = \left(Z/\beta\right) \int_{T_0}^{T} e^{-E_a/RT}\, dt \quad (3.68)$$

Then x – the conversion factor of the decomposed compound at time t, is expressed by equation 3.69

$$x = \frac{m_o - m}{m_0 - m_\infty} \quad (3.69)$$

Where m= mass remaining at time t, m_o= initial mass and m_∞ = final mass. Broido cited two estimates in literature by Horowitz and Metzger (1963). One is

$$e^{-E_a/RT} = \left(T_m/T\right)^2 e^{-E_a/RT} \qquad (3.70)$$

Where T_m is the temperature of peak reaction rate. Looking at the point that T_0 is usually much lesser than T_m, this estimate leads to

$$ln\left(Z/\beta\right)\int_{T_0}^{T} e^{-E_a/RT}\ dt \cong \frac{-E}{RT} + \ln\frac{RZT_m^2}{E_a\beta} \qquad (3.71)$$

the left-hand side of Equation (3.68) can only be integrated if *n=1* as follows:

$$\ln\left[\int_x^1 dx/x^n\right] = \ln\left[\int_x^1 dx/x\right] = ln\left[ln\left(1/x\right)\right] \qquad (3.72)$$

Combining Equations (3.68), (3.71) and (3.72), equation (3.73) can be obtained:

$$\ln\left(ln\frac{1}{x}\right) = \frac{-E}{RT} + \ln\frac{RZT_m^2}{E_a\beta} \qquad \text{for n = 1} \qquad (3.73)$$

Z is the frequency factor and Tm is the temperature of the maximum reaction rate Equation (3.73) is popularly known as the Broido method .Broido method is based on the postulation that the order of reaction is one(Broido A. 1969). The activation energy for the thermal degradation process is evaluated using simple form of Broido equation,

$$\ln\left(ln\frac{1}{x}\right) = \frac{-E}{RT} + \text{Constant} \qquad \text{for n = 1} \qquad (3.74)$$

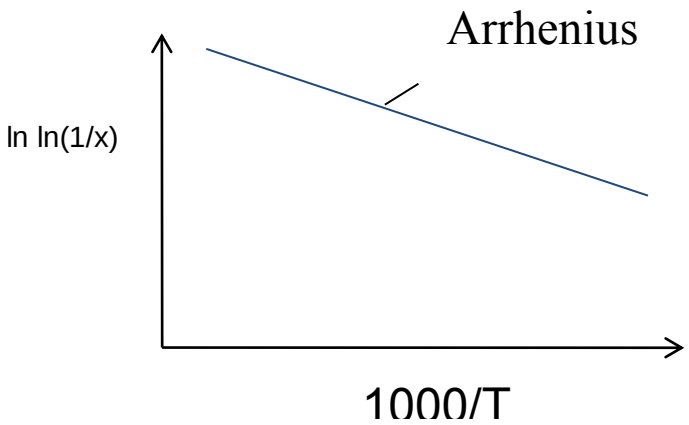

Figure 3.7: Rate coefficient against reciprocal temperature.

Broido method is ideal since there is no assumption made about the order of reaction.

3.6 Biodegradability

Biodegradation is the transformation of a substance into new compounds through biochemical reactions or the action of micro-organisms such as bacteria. For the degraded sheets in soil weight loss after a specified period is obtained by

$$W_{loss} = [(W_b - W_a)/W_b] \times 100\% \quad (3.75)$$

Where, W_{loss} is the weight loss, W_b and W_a are the weights of the dried out sheets initially and after degradation in soil within a specified period in days.

3.6.1 Biodegradation process

Biodegradation of polymers encompasses the subsequent stages; [Arutchelvi *et al.*, 2007];

(a) Attachment of micro-organisms to polymer surface.

(b) Growth of micro-organisms utilizing the polymer as the carbon source.

(c) Major degradation of the polymer.

(d) Final degradation.

Micro-organisms get on to the surface, if the polymer exterior is hydrophilic. As polypropylene has only CH2 groups, the surface is hydrophobic. Initial degradation leads to the insertion of hydrophilic groups on the polymer surface.

CHAPTER FOUR

MATERIALS AND METHODS

4.1 Materials

Virgin polypropylene with a density of 0.9g/cm^3 and a melt flow index of 30-70g/10min ,suitable for injection molding was obtained from Babadogo Premier Industries Kenya. The melt flow index is the measure of the resistance to flow of polymer melt at a given temperature under a given force for a given time. Figure 4.1 (a) shows PP pellets .The fiber was extracted from sausage fruit tree in Kyeni, Embu County which was investigated and identified by a Kenyatta university taxonomist as a fruit from sausage fruit tree. Figure 4.1 (b) shows the sausage fruit tree fiber

Figure 4.1 (a): PP pellets

Figure 4.1(b): sausage fruit tree fiber

4.1.1 Melting chamber

Sausage fruit tree fiber (the source of cellulose) was dried for 12 hours at 90 °C and grinded into fine powder then sieved with a sieve of one gauge. Cellulose powder was

mixed with molten polypropylene in the weight ratio of 0:10, 0.5:9.5, 1:9, 1.5:8.5 and 2:8 respectively. Polypropylene/ Sausage fruit tree fiber blends was put in a cylindrical melting chamber placed on a hot plate as shown in figure 4.2

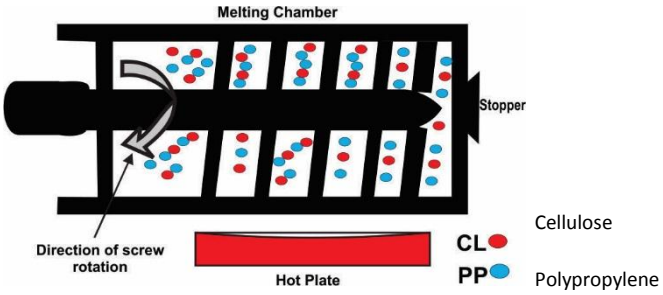

Figure 4.2: Melting chamber

The injection hole was closed by a stopper screw; the mixing screw was randomly rotated through 360^0 for 20 minutes to ensure that all the polypropylene melts evenly. Cellulose powder was added at 18^{th} minute and mixed for 2 minutes to obtain homogeneous mixture. The temperature in the melting chamber was selected at 189 °C (Korir P. Kiprono.2013). This temperature was selected in order to reduce the thermal degradation of cellulose blends extrusion and to achieve good cellulose dispersion in the matrix. Still hot, and the stopper screw removed the melt was quickly injected through the injection hole still hot at 189 °C into the circular disc molder which was at room temperature 25°C as shown in figure 4.3

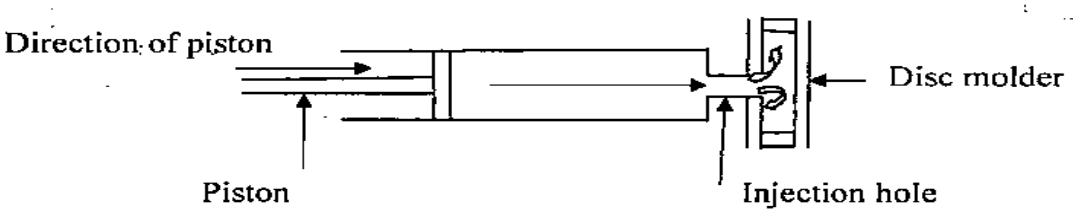

Figure 4.3: Injection molding process

4.1.2 Test samples

When cooled for about 3 minutes the mold took the shape of the circular disc molder. The mold is taken and film samples were cut along the flow direction (A) as shown in figure 4.4.

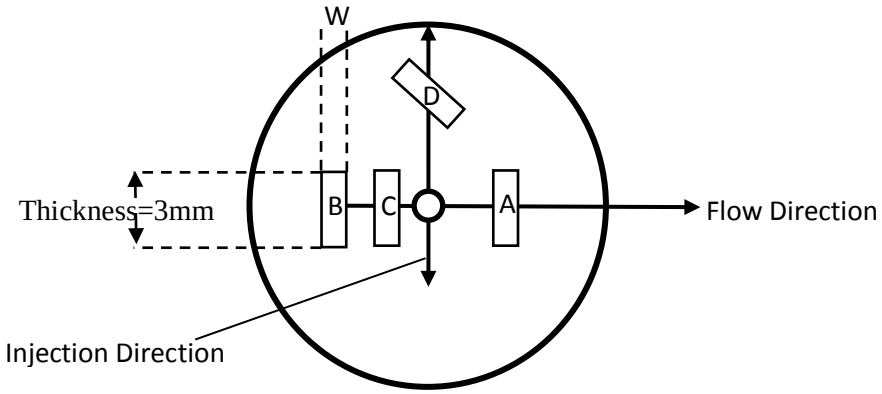

Figure 4.4: Nomenclature and dimensions of the sample

4.2 Measurements

The main measurements in this project were Dynamic mechanical analysis measurements, creep, Thermogravimetric analysis (TGA) and biodegradability. Diffusion measurements were made to provide information relating to sorption.

4.2.1 Dynamic mechanical properties

The dynamic mechanical properties were investigated using torsional pendulum in figure 4.5(Richards M.J.1971) at temperature range from 30 to 100 ^{0}C. Torsion is the twisting or wrenching of a body by the exertion of forces tending to turn one end or part about a longitudinal axis while the other is held fast or turned in the opposite direction on its own axis

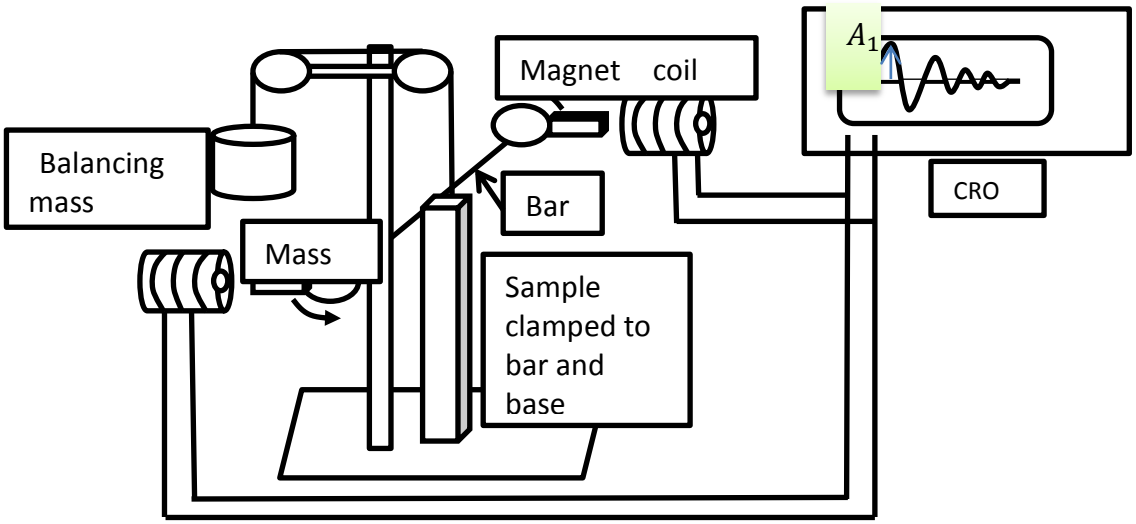

Figure 4.5: Schematic model of torsion pendulum

Mass of the metallic bar or beam was 641g while the mass of the balancing mass and the other masses attached to the bar (counter balancing) was 625g. Distance of separation between the masses was set to be 24cm. The CRO time base was set as 2.00 seconds.

To characterize this setup, pure polypropylene and high density polyethylene samples of dimensions about $(24 \pm 0.5) \times (12 \pm 0.5) \times (3 \pm 0.5)$ mm were used. Clamped and torsional oscillations induced manually then readings of amplitudes and periodic time obtained from CRO. The obtained value of storage modulus at 30^0C for pure PP was 32MPa within the theoretical range (31-45) MPa. The obtained value of storage modulus at 30^0C for HDPE was 15.2 MPa within the theoretical range (15-25) MPa.

The dynamic mechanical properties were investigated using the characterized torsional pendulum setup at temperature range from 30 to 100^0C for samples of pure PP and the bio-composites of dimensions about $(24 \pm 0.5) \times (12 \pm 0.5) \times (3 \pm 0.5)$ mm at different fiber loading. The varying storage modulus and the loss modulus were calculated.

storage modulus equation 3.11 becomes;

$$G' = \frac{l}{T^2} 64l \left(\frac{\pi}{wt}\right)^2 \qquad (4.\ 2.1)$$

Where T is the periodic time, l is the length, w the width and t the thickness of the sample.

Loss modulus is given by;

$$G'' = \frac{\Delta G'}{t} \qquad (4.2.2)$$

Where $\Delta = l_n \frac{A_1}{A_2} = l_n \frac{A_2}{A_3}$ is logarithmic decrement with A_1, A_2 , A_3 being the amplitudes from CRO.

4.2.2 Creep measurements

Recovery behavior and creep of the blends was evaluated using creep /recovery set up. Deforming mass of 200g was used. Creep measurements were performed at 30, 40, 50 and 60 °C. The time for deformation and recovery of the sample was maintained as 12 minutes (Korir P. Kiprono.2013). The samples of dimensions were about.$(24 \pm 0.5) \times (12 \pm 0.5) \times (3 \pm 0.5)$ mm were clamped as shown in figure 4.6 below

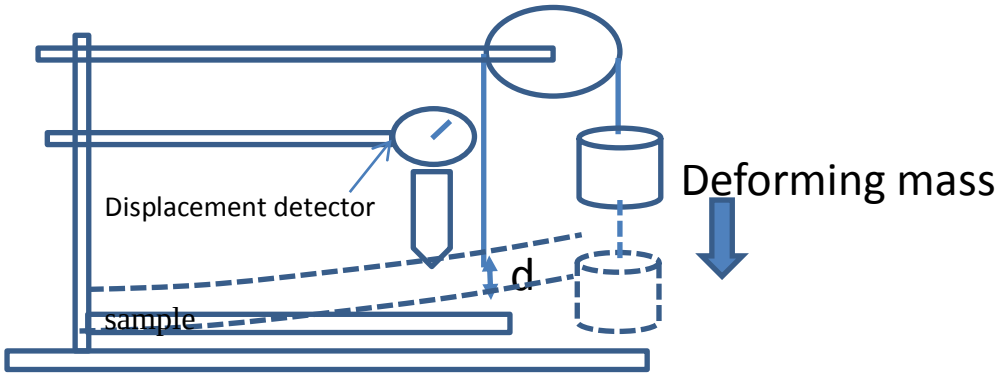

Figure 4.6: Stress applied by bending sample

To calculate the deflection / displacement (d), equation 4.2.3 below is used

$$displacement\ d = \frac{FL^3}{3EI} \quad (4.2.3)$$

Where, F is the force and the end point, L is the length of the sample, E is the creep or young's modulus and I is the moment of inertia. Moment of inertia here refers to the product of Force (F), applied and the perpendicular distance to the line of action of the force from the point of support (L). Creep modulus is given by $E = \frac{4F\ L^3}{d \times w \times t^3}$

Where w is the width of the sample and t is the thickness of the sample.

Bending stress is given by;

$$stress\ \sigma = \frac{6FL}{wt^2} \quad (4.2.4)$$

Creep is calculated using equation 4.2.5 below,

$$creep\ C = \frac{1}{E} \quad (4.2.5)$$

The setup was characterized by testing samples of dimensions $(24 \pm 0.5) \times (12 \pm 0.5) \times (3 \pm 0.5)$ mm of pure PP and HDPE at room temperature 25^0C. Young's modulus was calculated from equation 4.2.3 and found to be 1300Mpa for PP close to the theoretical value of 1325Mpa, while that of HDPE 750Mpa within the theoretical value range (600-1500Mpa)(Designer data,2019)

4.2.3 Diffusion measurements

The cut out samples of 0.121g of each composition were dried for 12 h at 50 °C, cooled and immediately weighed using an analytical balance until consecutive weighing gave same mass. Diffusion measurements were done by putting the samples in water at room temperature and studied after 7 days, 30 days, 60 and 90 days. The

samples were retrieved from the distilled water one by one, gently blotted with a cotton material to eliminate the excess of water on the surface, and weighed immediately to monitor mass difference for determination of water uptake. To get diffusion coefficient Fick's second law of diffusion was used.

4.2.4 Thermal stability

Thermo-gravimetric analysis (TGA) was carried out on samples of mass 0.1 g using Lindberg/Blue tube furnace TF55035C at 25 to 500 °C in order to determine the thermal behavior of the blends in oxidative environment at a heating rate of 20 °C /min. The initial and final degradation temperature and corresponding percentage weight loss for the samples were noted.

4.2.5 Biodegradability

The cut out samples of 0.124 g by mass of each composition were dried for 12 hours at a temperature of 50 °C, cooled and immediately weighed using an analytical balance until consecutive weighing gave same mass(Korir P. Kiprono.2013). Biodegradability of the PP/SFTF blends was carried out by using natural soil. The dried samples were covered up under soil in a hole dug about 20 cm deep in front of physics laboratory of Kenyatta University main campus. The average soil temperature and moisture content for the period sample burial was 25 – 27^{o}C and 60 – 70 % respectively. The soil pH was determined as 6.4 within the suitable soil pH range of 6.0 and 7.0 around which most bacteria grow best (Tarah .S Sullivan, 2017). Five degraded films were taken out one after 7 days, 30 days, 60 days and 90 days respectively, cleaned carefully, dried out in a vacuum for 24 hours at 50 °C and its mass measured until a constant mass was obtained.

CHAPTER FIVE

RESULTS AND DISCUSSION

5.1 Introduction

This chapter gives the experimental results obtained from storage modulus, 9loss modulus creep, diffusion, and TGA and soil burial test. Effect of fiber concentration on these properties are discussed

5.2 Dynamic mechanical analysis

Dynamic mechanical test methods investigate the viscoelastic behavior of polymers. Storage modulus, G' measures the stiffness of a material by determining its ability to absorb or store energy. High storage modulus implies the material is stiffer and this is a desirable quality. Loss modulus, G'' is the viscous response of a material. It is a measure of energy dissipated as heat per cycle under sinusoidal load.

5.2.1 Storage modulus and loss modulus

Figure (5.1) shows the variation of storage modulus G' with temperature for pure PP and PP-CEL blends at different loading.

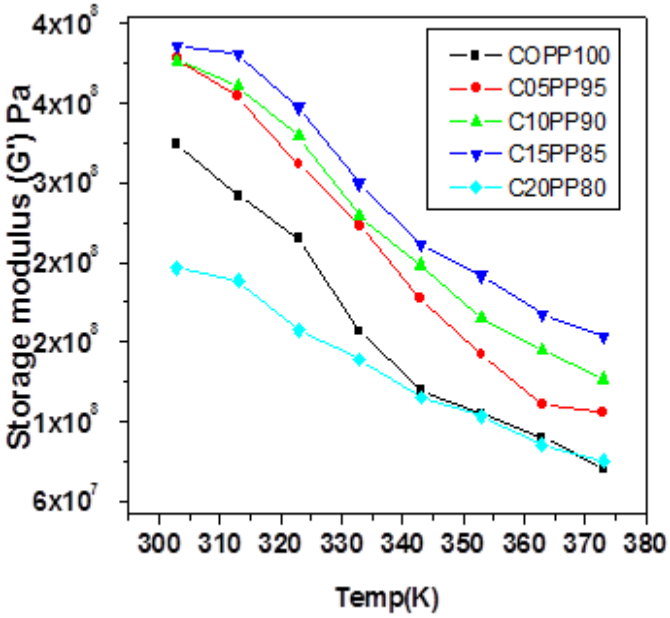

Figure 5.1: Storage modulus against temperature of PP and its cellulose blends.

A plot showing the variation of storage modulus with respect to temperature is shown in Figure 5.1. Storage modulus increases with cellulose loading particularly in comparison of C15PP85 with pure PP. Reinforcement imparted by the Sausage fruit tree fiber allows stress transfer from the matrix to the fiber. Introduction of the Sausage fruit tree fiber particles in the matrix gives better storage modulus hence stiffens the composite due to strong interactions between hydroxyl groups of STFF and PP chains. Increased storage modulus of the bio-composites suggests a better material and relatively good adhesion between the filler and the polymer. This is in agreement with a report on rice straw fiber polypropylene bio-composites where the storage modulus increased with fiber content (A. Grozdanov 2006) shown in figure 5.2

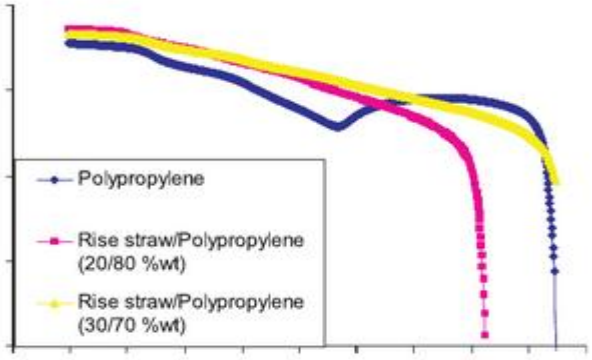

Figure 5.2: Storage modulus spectra of polypropylene and rice straw/ polypropylene composites

Blending PP with cellulose from acacia lowers the storage modulus (Korir P. Kiprono .2013). This affects the polymer negatively by making it less stiff. In this research beyond 15% SFTF loading, these interactions are briefly disrupted, softening the matrix which causes decrease in intermolecular bonding which lead to decrease in stiffness. As temperature increases storage modulus decreases due to reduction in stiffness or softening of the matrix at high temperature (Jawaid *et al.2011).*

Figure (5.3) shows the variation of storage modulus G' with temperature for pure PP and PP-CEL blends at different loading.

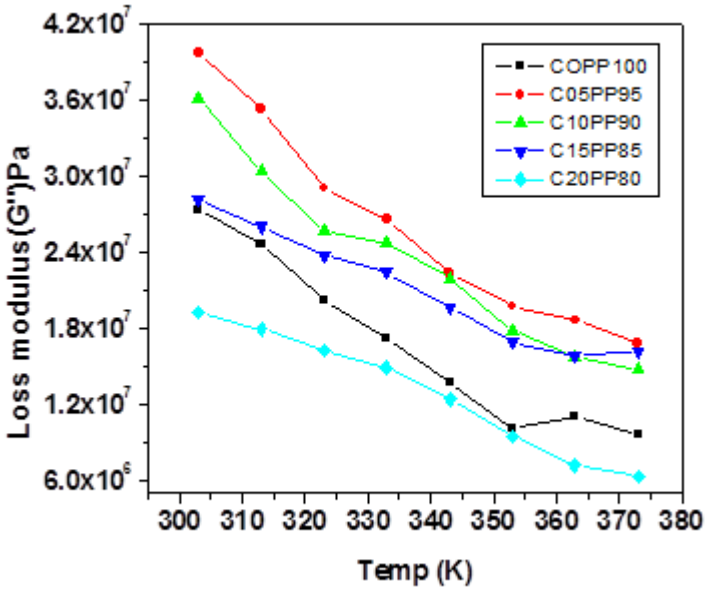

Figure 5.3: Loss modulus against temperature of PP and its cellulose blends.

Loss modulus is directly proportional to the energy dissipated either as heat or molecular rearrangements during loading cycles. It indicates the viscous nature of the polymer. It is observed that loss modulus found to generally increase with SFTF content with maximum loss modulus for C05PP95 in comparison with pure PP. Loss modulus then decreased to minimum for C20PP80 in comparison with pure PP this can be attributed to the reduced stiffness for C20PP80.. The incorporation of Sausage fruit tree fiber in the matrix improves the loss modulus due to decrease in the mobility of matrix.

5.3 Creep analysis

The presence of CEL changes volume fraction that affects the creep behavior of blends.

5.3.1 Percentage Strain and Recovery

Figure 5.4 shows the strain percentage as a function of time for pure PP and its cellulose blends.

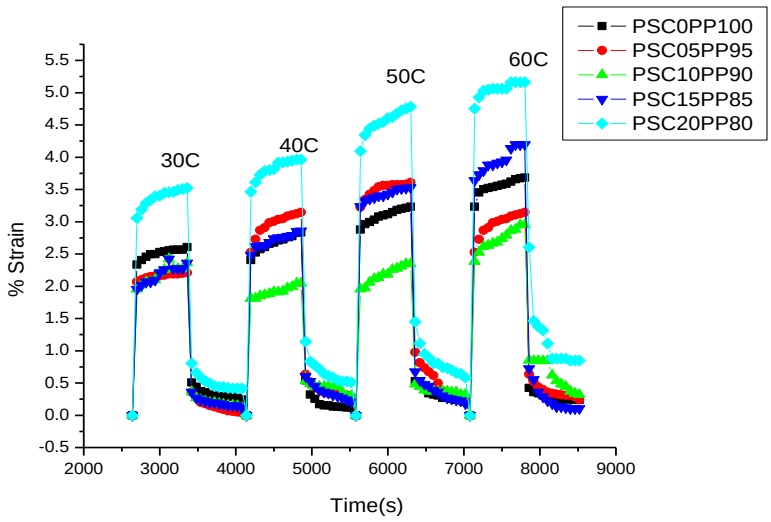

Figure 5.4: % creep strain of PP and its cellulose blends as a function of time at different temperatures.

It is observed from the results that as temperature increases, creep strain increase and material recovered. This is attributed to polymer chain mobility and less entanglement at elevated temperatures. It is also observed that increase in CEL led to increased deformation due to decreased resistance to creep. As temperature increases, Recovery decreased. Increase in CEL increased Recovery due to attraction caused by OH groups. Introduction of cellulose to the PP matrix also disturbs the structure hence affecting the recovery process. The structure recovers poorly but upon increasing cellulose intake, the recovery process increases.

5.3.2 Deformation -burger fit

Burgers model equation 3.14 was used to model creep deformation

$$\varepsilon(t) = \sigma_o\left(\frac{1}{E} + \frac{t}{\eta}\right) + \frac{\sigma_o}{E}\left(1 - e^{t/\tau}\right) = \frac{\sigma_o}{E_M} + \frac{\sigma_o}{E_k}\left(1 - e^{t/\tau}\right) + \frac{\sigma_o t}{\eta_M}$$

Where E_M the instantaneous elastic modulus, E_K is the delayed elastic modulus ,σ_0 is the constant applied stress, η_M is viscosity of the Maxwell element and η_K is viscosity of the kelvin dashpots are the fit parameters.

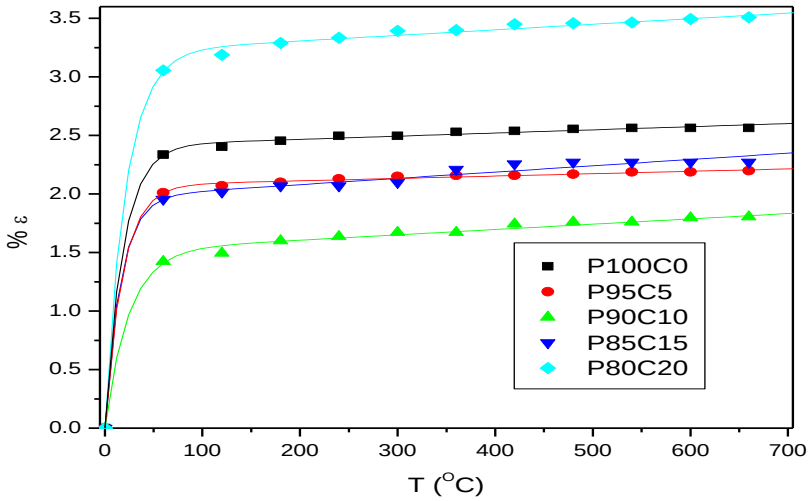

Figure 5.5: Burger fit master curves for deformation of PP and its cellulose blends

The parameters from the fit equation for the PP/SFTF blends are tabulated in Table 5.1 and it indicates that all of the four parameters demonstrate an increasing trend with the content of fiber

	Em(MPa) ±0.5	**Ek(MPa) ±0.05**	**$\eta m^{(x\ 10^{3}\ mpa\text{-}s)}$ ±0.05**	**$\eta k^{(x\ 10^{1}\ mpa\text{-}s)}$ ±0.5**
P100C0	35.3	1.29	5.54	20.0
P95C05	37.1	1.39	6.15	29.4
P90C10	39.3	1.56	8.26	30.0
P85C15	40.0	1.63	10.90	33.7
P80C20	45.6	1.18	8.20	35.2

Table 5.1: Burger fit four parameters for the PP/SFTF blends

Instantaneous creep strain that should be regained after withdrawal of load causing stress is given as $E_{M,}$ associated to the Maxwell spring. Increase in E_M up to 15 % fiber loading shows improvement in elasticity beyond which it decreases. The retardant elasticity E_k is associated with stiffness of polymer chains in short term. E_k increases up to 15 % fiber loading. This implies an increase in stiffness beyond which it decreases. n_K indicates the viscosity of the Kelvin–Voigt unit. n_K increases with cellulose loading implying increase in viscosity of Kevin-Voigt unit. Parameter n_M, signifies the irretrievable creep strain. The viscosity n_M rises with increase in cellulose hence lower flow and decreased permanent deformation. Weibull distribution expression was applied as following to mimic the recovery portion of the experimental data.

5.3.3 Recovery analysis-weibul fit

Weibull distribution expression 3.18 was applied to mimic the recovery portion of the experimental data.

$$\varepsilon_r(t) = \varepsilon_r \left[exp\left(-\frac{t}{\eta_r} \right)^{\beta_r} \right] + \varepsilon_f$$

Where β_r is shape parameter or Weibull slope, ε_r is strain after short time, ε_f is strain after long time ,η_r is characteristic life parameter. Figure 5.6 shows the Weibull fit master curves for PP and its cellulose blends

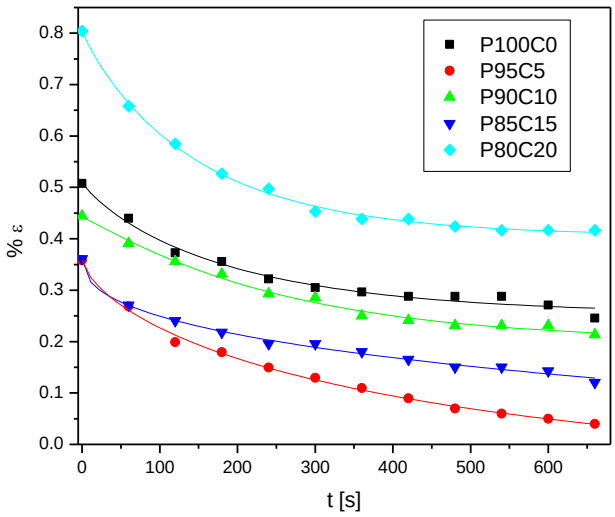

Figure 5.6: Weibull fit master curves for PP and its cellulose blends

The Weibull fit parameters obtained were tabulated in table 5.2 below

	ε_r ±0.05	η_r ±0.01	β_r ±0.02	ε_f ±0.05
P100C0	**2.41**	**2.89**	**0.23**	**0.20**
P95C5	**2.17**	**8.87**	**0.32**	**0.18**
P90C10	**1.65**	**5.12**	**0.20**	**0.15**
P85C15	**1.26**	**6.60**	**0.26**	**0.10**
P80C20	**1.11**	**6.21**	**0.29**	**0.08**

Table 5.2: Weibull parameters for the PP and its cellulose blends

The results show decrease of strain, ε_r and ε_f with % fiber loading indicates enhanced recovery performance. Characteristic life parameter, η_r and shape parameter, β_r increase with fiber loading intake. Shape parameter, β_r reflects change of failure rate of the cellulose composites. Generally adding cellulose cause a rise in viscosity, hence cellulose inhibits the slippage of molecular chains of polymer.

5.4 Thermogravimetric analysis

5. 4. 1 Thermogravimetric analysis of PP/CL blends

Thermal stability tests of PP-CEL blends is necessary in determining the temperature range of use in applications .TGA studies have been carried out to determine thermal stability and degradation temperatures of polypropylene and its cellulose blends. The

thermal degradation behavior of pure PP with various percentage of cellulose loading has been studied employing TGA and DTG thermograms as shown in Figure 5.7

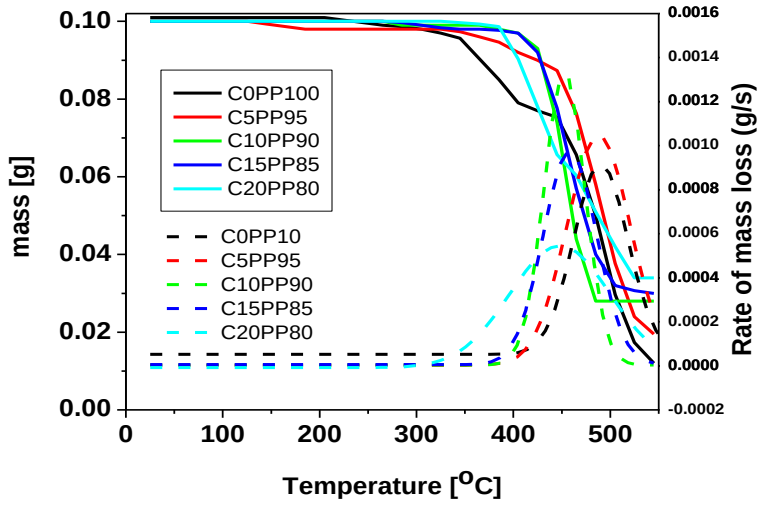

Figure 5.7: Thermogravimetric curves (lines) and derivative thermogravimetric curves (dotted) for PP and its cellulose blends.

Two stage decomposition was observed from the TGA graph. First-step (150-200^{o}C) represents removal of water from the matrix while the Second step represents decomposition of chain backbone and cellulose. The peaks of derivative thermogravimetric curves for PP and its cellulose blends gave the decomposition temperature of each sample, while the percentage mass residue was obtained by calculating the percentage of mass of remaining ash to the original mass of sample as shown in table 5.3

Sample	T_D (^oC) ±0.5	m_R (%) ±0.5
C0PP100	489.7	12.5
C5PP95	487.6	23.9
C10PP90	458.3	27.9
C15PP85	453.2	30.0
C20PP80	459.0	34.0

Table 5.3: Decomposition temperatures and % mass residue

DTG curves shifted to the left (decrease in decomposition temperature) with increase in CEL loading up to 15%. CEL. This agrees with report on acacia cel sap polypropylene bio-composites,as the cellulose concentration increases the decomposition temperature decreases from 478^0C for pure PP to 425^0C 20% cel loading for (Korir P. Kiprono et.,2013).

Decomposition temperature shifts to the right (increase in decomposition temperature) for 20% SFTF. Addition of fiber in the polypropylene cause strong CEL/PP interactions. At high temperatures these interactions are briefly disrupted by thermal vibration forces softening the matrix leading to a drop in decomposition temperature. However, at higher CEL loading, thermal vibration forces are overcome by strong CEL/PP interactions which stiffen the matrix again and decomposition temperature increases. The ash content increased with CEL loading. this implies Reduction of the production of toxic gases as reported by Dimitrova *et al*., 2008. Fiber in STFF/ PP retarded the degradation process or /and restricted diffusion of volatile degradation products out of the sample increasing the thermal stability.

Degradation of fiber in the composites was not observed as a separate step in the figure 5.7, indicating good interaction between fiber and PP.

5.4.2 Activation energy

Activation energy, E_a, is the least energy that molecules need to have so as to react to form a product. Linearly degenerated line of ln (ln(1/x)) versus 1000/ T was plotted as shown in Figure 5.8.

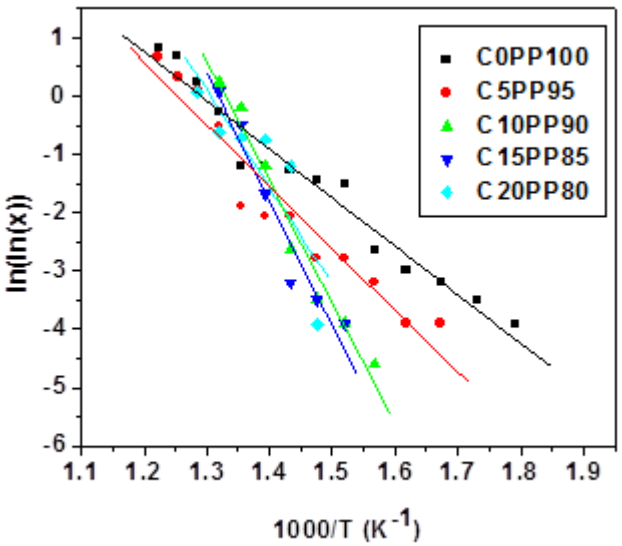

Figure 5.8: Natural logarithm of reciprocal residual mass versus reciprocal temperature of PP and its blend.

The activation energy was attained from the gradient of of ln (ln(1/x)) versus 1000/ T with reference to broido equation 3.74

$$\ln\left(ln\frac{1}{x}\right) = \frac{-E}{RT} + \text{Constant} \qquad \text{for n} = 1$$

Table 5.4 shows Activation energies of pure PP and its cellulose blends

Sample	Ea (KJ/mol) ±0.02
C0PP100	69.22
C5PP95	98.72
C10PP90	163.22
C15PP85	210.01
C20PP80	179.27

Table 5.4: Activation energies of pure PP and its cellulose blends.

Increase in activation energy of material implies increase in thermal stability of the material. Results obtained show that the thermal stability of SFTF- PP blends increases as the amount of cellulose increases. Highest activation energy is recorded for 15PP85 which implies highest thermal stability compared to other composite compositions.

Introduction of the Sausage fruit tree fiber particles stiffens the matrix due to strong CEL/PP interactions which implies more energy is required to decompose the material. This makes the SFTF/PP bio-composites better materials for application in external places exposed to high temperature .This was in agreement with report on rice straw fiber –PP composites that the rice straw/polypropylene composite showed slightly higher thermal stability; as the rice straw content increased, the thermal stability of the composites increased(A. Grozdanov 2006).

Acacia cel sap polypropylene bio-composites depicted a decreased trend of activation energies with pure PP having the highest E_a of 72.0 KJ/mol (Korir P. Kiprono et.,2013). This implied that this acacia sap polypropylene Bio-composites is poor materials in terms of thermal stability. Beyond 15% SFTF loading, the strong interactions are briefly disrupted by thermal vibration forces, softening the matrix leading to a drop in activation energy. The activation energy due to thermal decomposition of pure polypropylene (69.22 kJ/mol) is in agreement with the activation energy for pure PP of 61.8 and 66.7 kJ/mol reported by Al-Mulla *et al.* [2003] and Dimitrova *et al.* [2008] respectively using the Friedman's technique.

5.5 Diffusion

Pure PP exhibited good water resistance compared to PP-CEL blends. There was no noticeable water uptake in the first 7 days. Percentage weight gained by PP-CEL blends is attributed to water absorbed. It was observed that the blend exhibit higher diffusivity compared to pure PP. Water uptake increased with CEL loading as in figure5.9

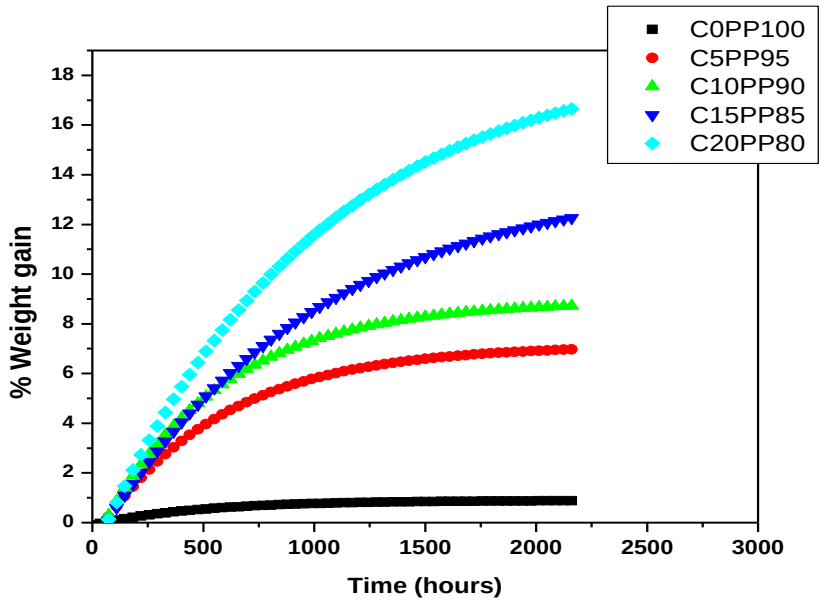

Figure 5.9: Variation of percentage weight of PP-CEL blends with time.

This is explained by the hydrophilic environment provided by CEL in the matrix. The percentage diffusant intake decreased with time and finally almost became constant. A similar trend was reported Korir P. Kiprono(2013) on water absorption behavior of polypropylene/acacia cel sap bio-composites

The reduction in the rate of water intake with time of stay in water could be attributed to concentration gradient through the sides of the sample. Initial water added to the composites strongly bonded with the hydrophobic cellulose fiber [Danjaji *et al.*, 2002]. Bhattacharya and Mani [1998] also argued that when water entered into the polymer blends and united with the OH groups, the cellulose pellets enlarged and abridged the space between their molecules. As the cellulose content rose, the particles congested and the gap became smaller and narrower. Thus diffusion of water became difficult and the rate of water intake reduced.

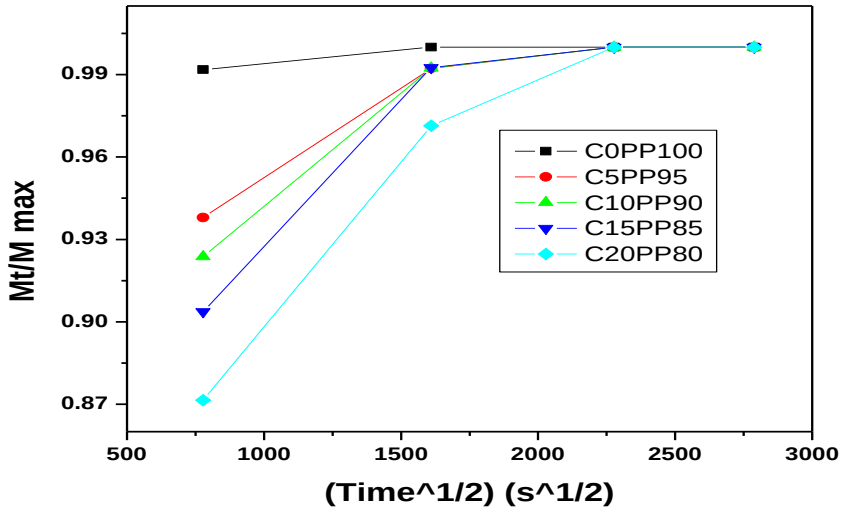

Figure 5.10: Fickian diffusion plots of Mt/M max versus t $^{1/2}$ for PP/SFTF blends

From Figure 5.10 the absorption curves are linear in the initial stages and above the linear portion the curves form a plateau. Plateau implies saturation almost occurred.

5.5.1 Diffusion coefficient

Water diffusion in to the blends is largely affected by CEL loading because water gets in to the matrix through the cellulose. To understand this concept of diffusivity, diffusion coefficient (D) was determined from linear initial curves of figure 5.10 that indicate that diffusion followed a Fickian process. ficks' second law equation 3.62 was employed

$$\frac{M_t}{M_{max}} = \frac{2}{l}\left(\frac{D}{\pi}\right)^{1/2} t^{1/2}$$

by determining the gradient of plot of M_t/M_{max} against t $^{1/2}$ for pure PP and its blends in water which is equal to $\frac{2}{l}\left(\frac{D}{\pi}\right)^{1/2}$ was used in calculating the diffusion coefficients given in the Table 5.5

Sample	D (cm^2/s) ±0.005
C0PP100	1.481×10^{-12}
C5PP95	8.990×10^{-11}
C10PP90	1.001×10^{-10}
C15PP85	1.370×10^{-10}
C20PP80	1.646×10^{-10}

Table 5.5: The diffusion coefficient for PP/ SFTF blends

Diffusion coefficient values increase with increase in cellulose loading. This agrees with results obtained by kahraman and Basel (2007), (A. Grozdanov 2006), (Korir P. Kiprono.2013). Diffusivity increases with cellulose intake due to polar hydroxyl groups in the matrix leading to hydrogen bonding with water molecules increasing water uptake. Hence, blending cellulose with polypropylene can improve the permeability of polypropylene material. As immersion time increased, water absorption rate decreased, this is explained by the fact that some CEL particles was leached away from the specimen (Ke et al.,2003).

5.6 Biodegradability

5.6.1 Biodegradability Results

Figure 5.11 shows the percentage mass loss as a function of time for the PP/CEL blends buried in the soil.

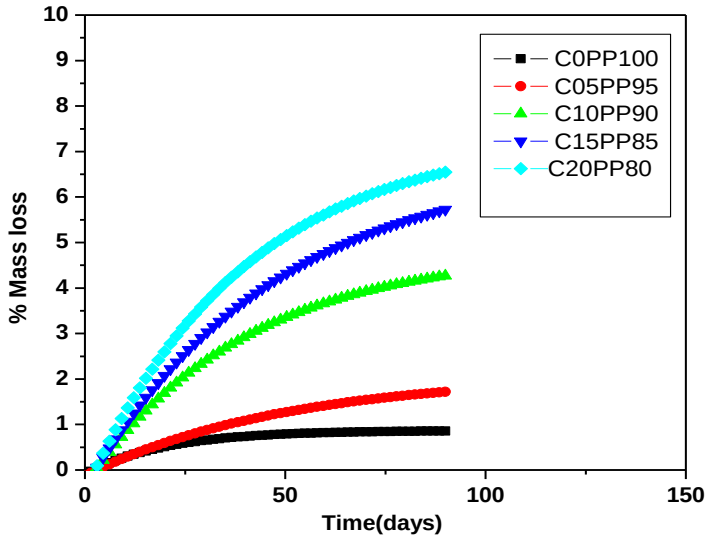

Figure 5 .11: % mass loss verses time in days for PP/ SFTF blends.

From the results, negligible percentage mass loss was noted for pure PP in other words, pure PP was not degraded. However, for PP/SFTF composites percentage mass loss increased. Degradation rate increased with CEL loading. This is in agreement with a report on polypropylene reinforced by cellulose fibers from rice straw that the weight of the pure PP was not changed after being buried in the soil for 50 days. However, the remaining weight of PP/CFs composites decreased with the burying time in the soil and their degradation rate increased with increasing CFs content (Ngo Dinh Vu ,2018).

Increased CEL gives microorganisms larger surfaces to consume hence higher degradation rate. First stage indicates high rate of biodegradation, attributed to the availability of highly polar hydroxyl groups in cellulose hence blend is more compatible with microorganisms. Second stage forms a plateau, attributed to the degradation of PP matrix. Exponential decay fit Regression lines were used to calculate full biodegradation period as shown in figure 5.12

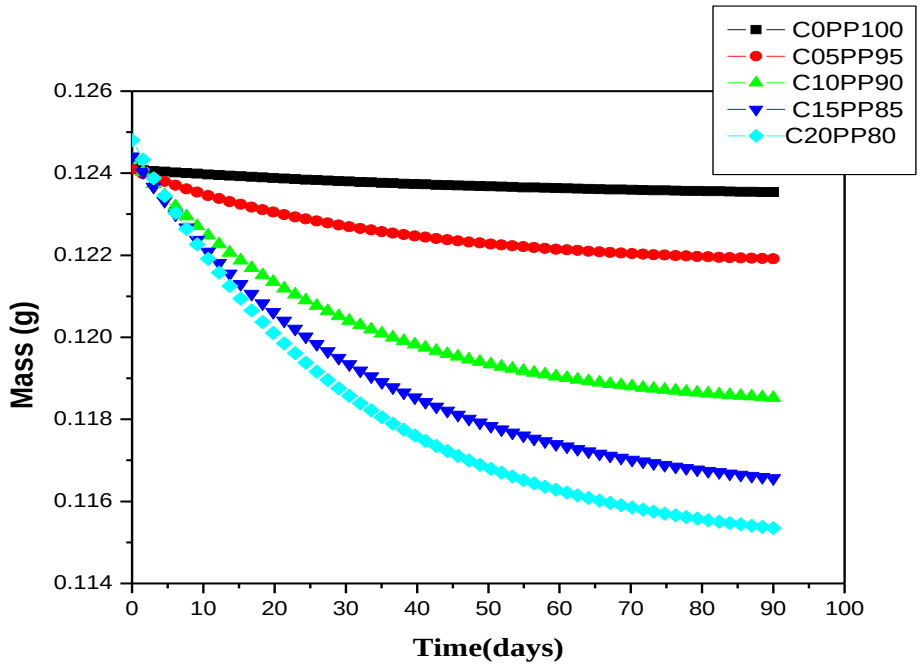

Figure 5.12: mass verses time exponential decay fit for PP/SFTF blends.

Rate of decay or degradation was determined using exponential decay formula equation 5.6.1

$$M_f = M_i \ e^{-kt} \qquad (5.6.1)$$

Where M_f is the final mass after degradation, M_i is the initial mass before degradation(Y intercept of figure 5.12), k is the rate of decay/degradation and t is the time of degradation in days. Logarithm property is used to linearize the experiment equation (5.6.1) in the form of equation of a straight line $y = mx + c$ to determine value of k for the different samples

$$ln\,(M_f) = -kt + \ln(M_i) \qquad (5.6.2)$$

Setting M_f at the lowest value equivalent to 0.1% of M_i, full degradation time in years was determined. Table 5.6 gives the rate of decay and lifespan of pure PP and SFTF/PP bio-composites.

Sample	Rate of decay$\times 10^{-5}$ (g/day) ± 0.5	Lifespan (Years)± 0.5
C0PP100	9.5	199.2
C5PP95	18.6	101.8
C10PP90	46.3	40.9
C15PP85	65.1	29.1
C20PP80	84.2	15.7

Table 5.6: rate of decay and life span of pure PP and SFTF/PP bio-composites.

Pure PP has the lowest Rate of decay or degradation. This is due to the presence of additives, antioxidants and other stabilizers Pure PP was resistant to biodegradation which make it toxic. It is also due to its hydrophobic structure consisting of extensive carbon chains that cause its' high resistance to hydrolysis (Khabbaz *et al.*, 2001). PP/ SFTF blends showed high Rate of decay or degradation with the highest rate at 20% fiber load .Various microorganisms consume the cellulose, which leave the PP matrix which has weakened bonding of polymer chains since Cellulose are more susceptible to microorganisms. This eases the breakdown of the material into minor portions. It also increases the external area open to oxygen. The outcome is that; the oxidation of PP turns out to be comparatively easy.

CHAPTER SIX

CONCLUSIONS AND RECOMMENDATIONS

6.1 Introduction

In this research, experiments and analysis of DMA, creep test, diffusion and degradability behavior of PP/ SFTF blends was done. This is a summary of the results, findings and analysis also suggests improvements required for future research works.

6.1.1 Conclusions

(i) The dynamic mechanical properties, the storage modulus and loss modulus were investigated as a function of temperature. These dynamic properties were influenced by the change in temperature and cellulose in the PP matrix. Storage modulus for pure PP sample is lower than its PP/ SFTF blends. Increase of SFTF in PP matrix led to increase in storage modulus due to the attractive effects of OH groups in cellulose that restricts the chain mobility stiffening the matrix. Loss modulus increased with increase in cellulose loading. This is attributed to by increased molecular environment participating in the relaxation process.

(ii) Percentage creep strain increased with increase in SFTF in PP matrix and led to increased deformation due to decreased resistance to creep. Increase in SFTF increased Recovery due to attraction caused by OH groups. Introduction of cellulose to the PP matrix disturbs the structure hence affecting the recovery process. The structure recovers poorly but upon increasing cellulose intake, the recovery process increases. The SFTF/PP bio-composite can with stand stress better than pure PP.

(iii) The values of activation energies increased with increase in SFTF loading indicating that the thermal stability of PP/ SFTF blends are higher than pure PP. Ash

collected at the end increased with SFTF loading. This shows that the toxic by-products decrease with increase in cellulose intake leading to less environmental pollution.

(iv) Fickian diffusion plots figure 5.10 show the diffusion of water followed Fickian process. The rate of uptake was greater with increase in cellulose content. Diffusion coefficient evaluated from the mass of water absorbed showed that the equilibrium uptake was directly proportional to the diffusion coefficient which increased from approximately 1.481×10^{-12} cm/s for pure PP to 1.646×10^{-10} cm/s for bio-composite at 20% fiber loading. Based on this study, it can be observed that the water diffusion in to the blends is strongly affected by quantity of cellulose.

(v) Biodegradability improved with cellulose loading. Availability of highly polar hydroxyl groups in cellulose which is more compatible with microorganisms leads to a great decrease in the mass of the sample that was buried under soil for the bio-composite with maximum decrease at 20% SFTF loading. Pure polypropylene showed negligible change in mass since it is hydrophobic in nature. The higher the content of cellulose in polypropylene matrix showed higher rate of decay than pure PP promising non-environmental pollutants. Rate of decay determined using exponential decay increased from 9.5×10^{-5} g/day for pure polypropylene to 84.2×10^{-5} g/day for bio-composite at 20% fiber loading. Lifespan of the bio-composites at 20% SFTF fiber loading is approximately twelve times less that of pure PP as in table 5.6.

From the conclusion it's clear that the mechanical, thermal, Biodegradability and diffusion properties of PP improved when SFTF cellulose is used as bio filler. Therefore PP/SFTF bio-composite developed has better properties for external applications and engineering. Being a biodegradable material it will help curb the problem of plastic landfills and also economically be an advantage to the society. For

instance the farmers who have the kigelia Africana tree in their farms will have an extra market for the fruits and by job creation in terms of collection of used sausage tree fruits from the brewers for fiber extraction.

6.1.2 Recommendations

Use of SFTF particles in polypropylene matrix should be adopted since these PP blends are promising non-environmental pollutants and diffusive membranes. Chemical treatment (alkali treatment) of the fiber may be adopted to reduce the diffusion coefficient in applications where diffusion is undesirable.

It would be necessary to carry out dynamic mechanical analysis for the PP/SFTF composites to investigate the storage modulus of the samples at high temperatures to get insight of the trend of stiffness at different fiber loading beyond 100^{0}C to around 550^{0}C. This may explain the T_D trend further. Use of X-Ray diffractometer to study the structure of these bio-composites may be useful to give insight on the molecular dynamics of the sample.

I would recommend a research at higher contents of SFTF in the PP matrix beyond 20% it may give more useful information about the properties of the bio-composite. This research used 20% SFTF as the optimum and recorded 15% SFTF to have the desirable properties, beyond which there was distortion.

These blends should be given a chance by policy makers in a bid to increase environment friendly polymers in the market and reduce on product cost since addition of cheap and locally available lignocellulosic waste product like sausage fruit tree fiber reduces on the cost.

REFERENCES

Alfonso, J. and Roxana, A. (2003). Polymer Degradation and Stability. *Journal of Applied Science,* **81** (2): 353 - 358.

A. Grozdanov(2006). Rice straw as an alternative reinforcement in polypropylene composites. Agronomy for Sustainable Development, Springer Verlag/EDP Sciences/INRA, 2006, 26 (4), pp.251-255.

Barbut, S. and Mittal, G. S. (1996). "Effects of three cellulose gums on the texture profile and sensory properties of low fat frankfurter"s. *Journal of Food Science and Technology*. **31**: 241-246.

Barrer, R. M. (1951). *Diffusion in and through Solids*. CUP Archive.

Bhattacharya, M. and Mani, R. (1998). Properties of injection molded starch/synthetic polymer blends-III. Effect of Amyclopectin to Amylase Ratio in starch. *European Polymer Journal*, **34**(10): 1467 - 1475.

Al-Mulla, A., Drozdov, A. D., Drozdov, D. A and Gupta, R. K. (2003). Thermal degradation and viscoelasticity of polypropylene-clay nanocomposites. *Polymer of Engineering Science,* **43**: 946 - 959.

Amash, A. and Zugenmaier, P. (1999). Morphology and properties of isotropic and oriented samples of cellulose fibre–polypropylene composites Polymer. *Polymer of Engineering Science,* **41** (4): 1589 - 1596.

Arutchelvi, J., Sudhakar, M., Ambika, A., Mukesh, D., Sumit, B. and Parasu, V. U. (2007). Biodegradation of polyethylene and polypropylene. *Indian Journal of Biotechnology*, **7**: 9 - 22.

Broge, J. L. (2000). Natural fibers in automotive components. *Automot. Eng. Int*, *120*.

Broido, A (1969). A simple, sensitive graphical method of treating thermogravimetric analysis data. *Journal of polymer science*, part A **27**:1761-1762.

Chandra, R. and Rustgi,R.(1998).Biodegradable polymers program polymer science.*Progress in polymer science* **23**:1273-1335.

Danjaji, I. D., Nawang, U. S., Ishiaku, H. and Mohd, Z. A. (2002*)*. Degradation studies and moisture uptake of sago-starch-filled linear low density polyethylene composites. *Polymer Testing and Stability,* **21**: 75 - 81.

Designer Data PP (En) [online] from

http://www.designerdata.nl/plastics/thermo+plastics/PP ?cookie=YES (n.d). [Accessed on 25 June 2019]

Dinh Vu, N., Thi Tran, H., and Duy Nguyen, T. (2018). Characterization of polypropylene green composites reinforced by cellulose fibers extracted from rice straw. *International Journal of Polymer Science, 2018*.

Dimitrova, A. S., Vlaer L. T., Turmannova, S. C. and Genieva, S. D. (2008). Non-isothermal degradation kinetics of filled with rice husk ash polypropylene composites. *Journal of Polymer Test,* **2:** 133 - 146.

Fancey, K. S. (2001). A latch-based weibull model for polymerie creep and recovery. *Journal of polymer engineering*, *21*(6), 489-510.

Fick, A. (1855). V. On liquid diffusion. *The London, Edinburgh, and Dublin Philosophical Magazine and Journal of Science*, *10*(63), 30-39.

Fuad, M. Y. A., Zain, M. J., Mustafah, J. and Ridzuan, R. (1994). Filler content determination of wood based composites by thermogravimetric analysis. *Journal of Polymer Test,* **13:** 15 - 214.

Gindl W. (2006)." Structural changes during tensile testing of an all-cellulose composite byin situ synchrotron X-ray diffraction*".Journal of composites science and technology*.66(**15**):2639-2647.

Guo, C., Song, Y., Wang Q. and Shen, C. (2006). Dynamic-mechanical analysis and SEM morphology of \voodflour/polypropylene composites. Harbin, China.

Ghasemi, E., and Kord, B. (2009). Long-term water absorption behaviour of polypropylene/wood flour/organoclay hybrid nanocomposite.

Hattotuwa, G. B., Premalal. H. I. and Baharin A. (2002). *Comparison of the mechanical - properties of rice husk powder filled polypropylene composites with talc filled polypropylene composites.*

Horowitz, H. H., and Metzger, G. (1963). A new analysis of thermogravimetric traces. *Analytical chemistry*, *35*(10), 1464-1468.

Jacobs, M. H., and Vietz, J. T. (1967). The basic processes affecting two-step ageing in an Al-Mg-Si alloy. *Philosophical magazine*, *16*(139), 51-76.

Jawaid, M., and Khalil, H. A. (2011). Effect of layering pattern on the dynamic mechanical properties and thermal degradation of oil palm-jute fibers reinforced epoxy hybrid composite. *BioResources*, *6*(3), 2309-2322.

Kahraman, R., and Abu-Sharkh Basel. (2007). Moisture absorption behavior of palm/polypropylene composites in distilled water and sea water. *International Journal of Polymeric Materials*, *56*(1), 43-53.

Ke, T., and Sun, X. S. (2003). Starch, poly (lactic acid), and poly (vinyl alcohol) blends. *Journal of Polymers and the Environment*, *11*(1), 7-14.

Kiprono, K. P. (2013). Mechanical, diffusion and degradation behavior of polypropylene and cellulose blends. *School of Pure and Applied Sciences of Kenyatta University, Nairobi City*.

Khalid, M., Ratnam, C. T., Luqman, A C., Salmiaton1,3 A., Choong, T. S. Y. and Jalaludin H. (2009). Thermal and Dynamic Mechanical Behavior of Cellulose and Oil Palm Empty Fruit Bunch (OPEFB)-Filled Polypropylene Biocomposites. *Journal of Polymer-Plastics Technology and Egineering,* **48** (12): 1244 - 1251.

Khabbaz, F., Albertsson, A. C. and Karlsson, S. (2001). "Rapid test methods for analyzing degradable polyolefins with a proxidant system". *Journal of Applied Polymer Science,* **79**: 2309 - 2316.

Lenntech,B.V(1998).*Water treatment and purification holdings*

Ljungberg, N., Cavaille, J-Y. and Heux, L. (2006). *Nanocomposites of isotactic polypropylene reinforced with rod-like cellulose whiskers.* Grenoble. France.

Park, B. D. and Balatinecz, J. J. *(*1997*).* The Effects of Temperature and Moisture on the Properties of Wood Fiber Thermoplastic Composites. *Journal of Thermoplastic Composites,* **10**: 476 - 487.

Reddy,N.and Yang,Y.(2005).*Properties and potential applications of natural cellulose fibers fron cornhusks.Effect of different coupling agents on the browning of cellulose-polypropylene composites during melt processing*. Green chemistry,**7**(4):190-195.

Richards ,M.J.(1971).An ABC of dimensional analysis. Physics ed.

Rongbo,L.,Xiuqin,Z.,Ying,Z.,Xuteng,H.,Xutao,Z.and Dujin,W.(2009).*New polypropylene blends toughened by polypropylene/poly(ethylene-co-propylene)in*

reactor alloy: Compositional and morphological influence on mechanical properties. Harbin,China

Roylance, D. (2001). Engineering viscoelasticity. *Department of Materials Science and Engineering–Massachusetts Institute of Technology, Cambridge MA, 2139*, 1-37.

Selke, S. (2000). *Plastics recycling and biodegradable plastics.* pp. 12-16

Sullivan, T. S., Barth, V. P., and Lewis, R. W. (2017). *Soil acidity impacts beneficial soil microorganisms*. Washington State University Extension.

Várdai. R (2019). Impact modification of PP/wood composites: a new approach using hybrid fibers. Express Polym Lett 2019; 13: 223–234.

Westerhout, R. W. J., Waanders, J., Kuipers, J. A. M. and Van, W. P. M. (1997). Experimentation and evaluation of the use of screen heaters for the measurement of the high temperature pyrolysis kinetics of polyethene and polypropene. *Journal of Industrial and Engineering Chemistry Research,* **36**: 3360 - 3368.

Yang, J. L., Zhang, Z., Schlarb, A. K. and Friedrich, K. (2004). Resistance to time-dependent deformation of nanoparticle/polymer composites. *Polymer Science and Technology,* **45**: 3481.

APPENDIXES

APPENDIX I: Photograph of Torsional pendulum system.

APPENDIX II: Photograph of Creep/recovery measurement set up.

APPENDIX III: Photograph of complete TGA system(Lindberg/blue tube furnace)

APPENDIX IV: Photograph of sausage fruit tree (Muratina-in gikuyu)